Available online at www.sciencedirect.com
SCIENCE DIRECT®
International Journal of Thermal Sciences 42 (2003) 107–140
International Journal of Thermal Sciences
www.elsevier.com/locate/ijts

Review of saturated flow boiling in small passages of compact heat-exchangers

Barbara Watel [1]

CEA-Grenoble/DTP/GRETH, 17, rue de Martyrs, 38054 Grenoble cedex 9, France

Received 9 July 2001; accepted 8 March 2002

Abstract

Intensification of process heat exchangers has led to considerable interest in compact heat exchangers for evaporation. These heat exchangers are characterised by multichannel passages with hydraulic diameters less than about 10 mm. In this article, two different categories of channels composing compact heat exchangers are reviewed: small circular and rectangular channels (including studies of individual channels and multichannel arrangements of parallel channels) and multichannel arrangements of straight perforated and serrated fin passages. The regimes of the two-phase flow which occur in these passages differ from those in larger systems. The typical trends of local heat transfer coefficient in small passages of compact heat exchangers show that it is easy to distinguish between the two dominant mechanisms of boiling, nucleate and convective boiling. The insights relative to heat transfer mechanisms in small passages and the flow patterns associated to convective and nucleate boiling regions are presented. In particular, the effects of vapour quality, mass flux, heat flux, channel geometry/size, fin type, gravity and surface tension in each boiling region are highlighted. Literature correlations valuable in small channels expressing the local boiling heat transfer coefficient as a function of vapour quality, mass flux, heat flux, fluid properties, fluid pressure and channels dimensions are reported.

Keywords: Flow boiling; Two-phase flow; Convective boiling; Nucleate boiling; Compact heat exchanger; Multichannel; Heat transfer coefficient; Fins; Small channels; Flow patterns

1. Introduction

Over the past decade, compact heat exchangers have been used more and more widely in applications involving phase changes, mainly due to their multistream capabilities, high thermal efficiencies, small size, low weight, design flexibility and energy savings [1–10]. Unlike shell-and-tube heat exchangers, compact heat exchangers can be designed to operate in a pure counterflow mode and can accommodate multiple fluid streams. They allow a reduction in the quantity of the fluid in the evaporator with a subsequent increase in safety and, in the case of refrigeration systems, an increase in environmental acceptability. Their reduced physical size leads to less material being used in their manufacture and in the construction of associated equipment and buildings. Energy savings result from the reduction in heat losses and the greater heat exchanger effectiveness obtainable. Recently there has been a growing awareness of the benefits of process intensification, the reduction in plant size, for a given capacity, by an order of magnitude or more, and this has led to a requirement for smaller evaporators [9,10]. In this article, two different categories of channels composing compact heat exchangers are reviewed: the small circular and rectangular channels (including studies of individual channels and multichannel arrangements of parallel channels (Fig. 1)), and the multichannel arrangements of straight perforated and serrated fin passages (Fig. 2). In the latter configuration, internal sub-channels are formed within the corrugated finning which spans the flat plates separating adjacent streams. Research on nucleate boiling in confined spaces is also reviewed in relationship to phenomena occurring in compact heat exchangers.

Compact heat exchangers have traditionally found wide application in the transportation industry, where they are used as evaporators and condensers in vapour-compression cycles for refrigeration and air conditioning [5,6,10,11]. Today, there is widespread interest in expanding the range of

E-mail address: barbara.watel@ujf-grenoble.fr (B. Watel).
[1] Maître de Conférences à l'Université Joseph–Fourier de Grenoble.

1290-0729/02/$ – see front matter
PII: S1290-0729(02)00013-3

Nomenclature

a	thermal diffusivity ..... $m^2 \cdot s^{-1}$
Bo	$= \dot{q}/(\dot{m}L_v)$, boiling number
Ca	$= \mu_L \dot{m}(x/\rho_V + (1-x)/\rho_L)/\sigma$, capillary number
CHF	critical heat flux (heat flux required to initiate dryout) ..... $W \cdot m^{-2}$
Co	$= [\sigma/\{g(\rho_L - \rho_V)\}]^{0.5}/D_h$, confinement number
Co_{Shah}	$= [(1-x)/x]^{0.8}(\rho_V/\rho_L)^{0.5}$, convection number
c_p	specific heat ..... $J \cdot kg^{-1} \cdot K^{-1}$
D	tube diameter ..... m
D_h	(= 4 flow area/wetted perimeter), hydraulic diameter ..... m
D_{hp}	(= 4 flow area/heated perimeter), hydraulic diameter based on heated perimeter ..... m
E	enhancement factor for the enhancement model
F	$= \alpha_{cv}/\alpha_L$, convective enhancement factor defined by ratio of the two phase coefficient to that for the liquid phase flowing alone
f	Fanning friction factor
Fo	$= a_{\text{L}}/(Ns^2)$, Fourier number
Fr	$= \dot{m}^2/(\rho_L^2 g D_h)$, Froude number
h	fin height ..... m
j_V^*	$= \dot{m}x\rho_V^{-1/2}[gD_h(\rho_L - \rho_V)]^{-1/2}$), modified Froude number
L_f	interruption length (offset-strip fins) ..... m
L_v	latent heat of vaporisation ..... $J \cdot kg^{-1}$
M	molecular weight ..... $g \cdot mol^{-1}$
$\dot{m}$	mass flux ..... $kg \cdot m^{-2} \cdot s^{-1}$
N	emission frequency of coalesced bubble ... s^{-1}
n_{pm}	number of fins per meter
Nu	$= \alpha D_h/\lambda$, Nusselt number
p	pressure ..... Pa
p_{red}	$= p/p_{\text{cr}}$, reduced pressure
Pr	$= \mu c_p/\lambda$, Prandtl number
$\dot{q}$	heat flux ..... $W \cdot m^{-2}$
R_a	wall roughness ..... m
Re	$= \dot{m}D_h/\mu$, Reynolds number
Re_L	$= \dot{m}(1-x)D_h/\mu_L$, liquid-phase Reynolds number
Re_{TL}	$= \dot{m}D_h/\mu_L$, Reynolds number of total flow regarded as liquid
Re_V	$= \dot{m}xD_h/\mu_V$, vapour-phase Reynolds number
S	suppression factor
s	fin spacing, clearance of a space ..... m
T	temperature ..... K
X	$= (\Delta p_{F,L}/\Delta p_{F,V})^{1/2} = [(f_L/f_V)(\rho_V/\rho_L)]^{1/2} \times (1-x)/x$, Martinelli parameter (general definition)
X_{tt}	$= [(f_L/f_V)(\rho_V/\rho_L)]^{1/2}(1-x)/x$, Martinelli parameter for the particular case where the liquid and vapour phases are turbulent
x	vapour quality

Greek symbols

α	heat transfer coefficient ..... $W \cdot m^{-2} \cdot K^{-1}$
α_{cv}	convective boiling heat transfer coefficient ..... $W \cdot m^{-2} \cdot K^{-1}$
α_L	heat transfer coefficient for the liquid phase flowing alone (based on $\dot{m}(1-x)$) $W \cdot m^{-2} \cdot K^{-1}$
α_{nb}	nucleate boiling heat transfer coefficient ..... $W \cdot m^{-2} \cdot K^{-1}$
α_{TL}	heat transfer coefficient for the total mass flow rate $\dot{m}$ flowing as a liquid ..... $W \cdot m^{-2} \cdot K^{-1}$
Δp_F	frictional pressure drop on flow length Δz; liquid phase flowing alone ($\Delta p_{F,L} = 2f_{\text{L}}\dot{m}^2(1-x)^2\Delta z/(\rho_{\text{L}}D_{\text{h}})$), vapour phase flowing alone ($\Delta p_{F,V} = 2f_{\text{V}}\dot{m}^2x^2\Delta z/(\rho_{\text{V}}D_{\text{h}})$) ..... Pa
ΔT_{sat}	$= T_w - T_{\text{sat}}$, difference between the wall temperature and the saturation temperature .. K
Δz	flow length ..... m
δ	fin thickness ..... m
λ	thermal conductivity ..... $W \cdot m^{-1} \cdot K^{-1}$
μ	dynamic viscosity ..... $Pa \cdot s^{-1}$
ρ	density ..... $kg \cdot m^{-3}$
σ	surface tension ..... $N \cdot m^{-1}$

Subscripts

cr	critical
L	liquid properties, or corresponding to liquid portion flowing alone in the channel
$L0$	corresponding to entire flow as liquid
sat	saturation
tr	transition between the two boiling regions
tt	corresponding to turbulent liquid and vapour flow
V	vapour properties
w	wall

application of compact heat exchangers to include phase-change heat transfer in chemical process industries, among others [1,2,5–7,11–14]. In particular, applications of compact evaporators and condensers include control of temperature-sensitive processes, diabatic distillation, hydrocarbon separation, cryogenic processing systems for liquefaction of gas (nitrogen, helium, natural gas) and the separation of oxygen and nitrogen. There are also a number of actual and potential applications in which a compact heat exchanger passage geometry is needed to facilitate highly-efficient heating or cooling process involving boiling or condensation. Instead of heat transfer between two streams, these ap-

plications may involve transport of heat to or from a condensing or evaporating stream due to its proximity to a continuous source or sink of thermal energy. Applications of this type may include condensation in passages of spacecraft radiator panels, vaporisation of coolants in cold plates for electronics cooling in the field of microelectronics, vaporisation in coolant passages in fusion reactor walls, thermal control of avionics in high-performance military aircraft, thermal control of spacecraft payloads [5,15–19]. In the case of nuclear engineering, narrow channels can be used in plate-type nuclear fuel element cooling. They are encountered in high conversion nuclear reactors, liquid metal cooled reactors and high flux research reactors [1,2,16,19,20]. For instance, in high conversion pressurised water reactors, distances between rods in fuel bundles can be as narrow as 1 mm. Due to the urgent needs for cooling electronic components and devices, microscale heat transfer technologies such as mini heat exchangers with flow channels having dimensions ranging from the order of several hundred to 0.1 μm have been developed. These microchannels and mini heat exchangers have also found their application in reactors for modification and separation of biological cells, selective membranes and liquid/gas chromatographies [17,18].

The operating conditions within the small passages of compact heat-exchangers are also very dissimilar to those in other forms employing, for example, large round tubes. There are several features of the operating characteristics of compact surfaces in vaporisation and condensation applications that strongly affect how they will perform. First, compact heat-exchangers are characterised by a small passage hydraulic diameter of a few millimetres and a very large surface-area-to-volume ratio (>700 $m^2 \cdot m^{-3}$ according to Shah [21]). The second important operating feature relates to the complexity of the passage and its impact on pressure drop [5]. Complexities in phase-change heat transfer are also due to the fact that compact evaporators and condensers typically operate through the laminar, transition and turbulent flow regimes. Moreover, the flow regimes present in small channels have been observed to differ from those in large channels [22]. In phase-change heat transfer in compact heat exchangers, in addition to fluid properties, heat flux, mass flux and vapour quality, the major parameter that can have a direct effect on the heat transfer coefficient and two-phase flow phenomena is channel geometry and size [3]. The operating conditions (mass and heat fluxes) depend on the type of compact heat exchanger and its application. For example, operation of compact plate-fin heat exchangers is usually associated with cryogenic plants. Therefore, the features of the design which reflect the operational requirements of cryogenic plant are the very low temperatures differences of the order of a few Kelvin between process streams, and the concomitant low heat fluxes (lower than 4 $kW \cdot m^{-2}$). Moreover, to avoid excessive pressure drop of the evaporating fluid, mass fluxes in finned passages are often less than 100 $kg \cdot m^{-2} \cdot s^{-1}$ [5,12,13]. According to Wadekar [23], generally industrial reboilers operate at moderate exit qualities and at low to moderate mass fluxes, where convective heat transfer associated with slug and churn flow is susceptible to dominate. The heat transfer characteristics under these conditions are significantly different from those exhibited at higher quality and higher mass flux. At the opposite of plate-fin heat exchangers, according to Wambsganss et al. [24], Tran et al. [25], in compact heat-exchangers comprising small multichannels operating in parallel, the higher heat transfer surface area density inherent in compact heat exchangers allows attainment of significantly higher heat flux levels in two-phase flows relative to conventional circular tube exchangers. Cornwell and Kew [3], Wambsganss et al. [24] also underlined that to avoid unacceptably high pressure drops, the small channel cross section led to low mass fluxes with Reynolds numbers typically in the laminar regime for the subcooled liquid.

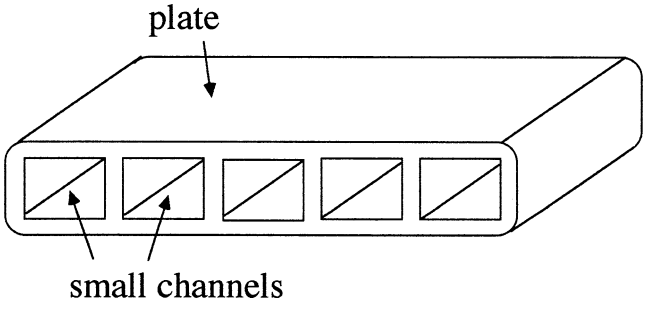

Fig. 1. Diagram of multichannel arrangement consisting of plate with parallel small channels.

Compared to gas–liquid flow in large channels or single-phase flow in compact heat-exchangers, fewer data relating to two-phase flow and boiling heat transfer in compact

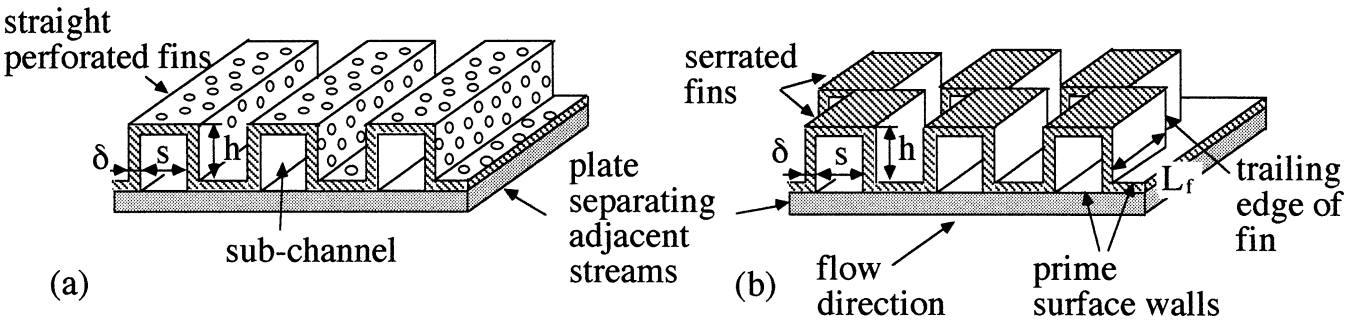

Fig. 2. Diagrams of typical straight perforated (a) and serrated (b) fin passages.

heat exchangers are available. A significant barrier to the application of compact evaporators and condensers in the process industries is the lack of validated design correlations to predict the heat transfer coefficient and an industrial standard. The development of design correlations requires an accurate data base, a knowledge of the prevailing flow regimes and the understanding of relationship between flow and heat transfer and of the physical mechanisms involved. With regard to the physical mechanisms of heat transfer, it is important to know whether the dominant heat transfer mechanism is forced convection or nucleation, and for what range of pertinent parameters each mechanism is dominant. This importance stems from the fact that the analyst must know and understand the mechanisms to appropriately model and correlate the heat transfer data, while the designer must know the dominant mechanism in order to appropriately apply the design correlations available to him.

In the present work, first experimental studies on flow boiling considered to be pertinent to compact heat exchangers are presented by giving for each study channel geometry/size, test conditions and fluids used. Then, the different flow pattern configurations susceptible to be observed during flow boiling in small passages of compact heat exchangers are enumerated, paying attention to the effect of different parameters such as channel dimensions. By referring to the results of previous researches, the typical trends of heat transfer coefficient in the two regions of boiling, nucleate and convective boiling regions are presented as well as the tools to distinguish between the two mechanisms of flow boiling and operating conditions at transition between both boiling regions. Then, basing on the results of different experimental studies, the objective of the present article is to analyse the heat transfer characteristics and associated flow patterns in the small passages of compact heat exchangers in each boiling region separately. In particular, the effects of vapour quality, mass flux, heat flux, channel geometry/size, gravity and surface tension in each boiling region are highlighted. Some interesting correlations to predict the boiling heat transfer coefficient formulated by researchers, valuable in channels of small dimensions, in the nucleate or convective boiling regions, are reported in the last part of the article.

2. Presentation of experimental studies

Studies of saturated flow boiling in small passages of compact heat exchangers can be categorised according to studies of multichannel arrangements of compact plate-fin heat exchanger passages (with offset strip or perforated fins) and small, circular and rectangular channels. Most of these studies are reviewed afterwards. Some experimental studies on nucleate boiling in confined spaces considered to be pertinent to compact heat exchangers are also reviewed.

2.1. Presentation of experimental studies in multichannel arrangements of straight perforated and serrated fin passages

The fin geometries, test conditions and fluids used in experimental researches on the determination of boiling heat transfer coefficients in multichannel arrangements of compact plate-fin heat exchanger passages are summarised in Table 1. In the first studies, only overall heat transfer coefficients in compact heat exchangers with offset-strip or perforated fins were determined from global measurements [26–30]. In more recent studies in compact offset-strip and perforated fin heat exchanger passages (Robertson, Wadekar and co-workers at Heat Transfer and Fluid Flow Services (HTFS) and Carey and co-workers at the University of California-Berkeley), local boiling heat transfer coefficients (i.e., at given axial positions) were measured and presented against vapour quality, over a large range of vapour quality, mass and heat fluxes.

In the studies of Robertson, Wadekar and co-workers, the fin passages were formed by the finning sandwiched between two aluminium side-plates. The test section was representative of a portion of one channel of a plate-fin heat exchanger. It was heated by electrical heaters producing a reasonably uniform heat flux on the inner faces of both aluminium side plates in contact with the test fluid. Moreover, the ranges of operational parameters used in their experiments (low mass and heat fluxes) were representative of industrial applications in the chemical process industry. Robertson [12,31] and Robertson and Clarke [32] analysed the variation of local convective boiling coefficients with vapour quality, mass flux and pressure, from tests with liquid Nitrogen in vertical channels with perforated and serrated fins. Robertson and Lovegrove [13, 33] measured the local boiling coefficients of Freon 11 in a vertical serrated plate-fin passage. Robertson and Wadekar [34] and Wadekar [4] reported their findings about boiling heat transfer characteristics of cyclohexane and heptane respectively against vapour quality and mass flux in a vertical perforated plate-fin passage at a low pressure of 150 kPa.

Carey and his co-workers [1,2,35] studied single-phase and flow boiling heat transfer of different fluids in offset-strip fins test sections made up of copper slabs. The test section was electrically heated on one side with an adiabatic glass-plate cover on the other side to allow for visualisation of the boiling process and associated flow patterns. Tests were performed with the test section oriented horizontally [35] as well as vertically [1,2]. They reported the single-phase and local boiling heat transfer coefficients on the heated portion of the channel against vapour quality, for different mass fluxes. It should be noted that the aspect ratios of the passages were not typical of compact plate-fin heat exchangers.

Koyama et al. [36] experimentally investigated the characteristics of heat transfer and flow patterns on the falling

Table 1
Summary of research studies with multichannel arrangements of straight perforated and serrated fin passages

Researcher(s)	$L_f/h/\delta/s$ (mm)	n_{pm}	D_h (mm)	$\dot{m}$ (kg·m^{-2}·s^{-1})	$\dot{q}$ (kW·m^{-2})	Superheat (K)	Fluids	Form of fins	Orientation/Heating	p_{sat} (kPa)
Robertson [12]	3.18/6.15/0.2/1.49	591	2.4	11–110	<4	0.4–1.5	Nitrogen	Offset-strip	Vertical upflow Both sides electrically heated	300
Robertson [31]	−/6.15/0.2/1.49	590	2.4	37–120	<4		Nitrogen	Perforated	Vertical upflow Both sides electrically heated	140–520
Robertson and Clarke [32]	−/6.15/0.2/1.49	590	2.4	37–0120	<4		Nitrogen	Perforated	Vertical upflow Both sides electrically heated	140–500
Robertson and Lovegrove [13,33]	3.18/6.15/0.2/1.49	591	2.4	34–159	<4	0.5–1.5	R11	Offset-strip	Vertical upflow Both sides electrically heated	300–700
Robertson and Wadekar [34]	−/6.15/0.2/1.49	590	2.4	50–290	1–10		Cyclohexane	Perforated	Vertical upflow Both sides electrically heated	150
Wadekar [4]	−/6.15/0.2/1.49	590	2.4	50–290	<4	0.5–1.7	n-heptane	Perforated	Vertical upflow Both sides electrically heated	150
Carey and Mandrusiak [1]	12.7/3.8/1.59/7.93	105	5.14	3–100			Methanol, butanol and water	Offset-strip	Vertical upflow One side electrically heated	100
Mandrusiak and Carey [2]	12.7/3.8/1.59/7.93 12.7/9.52/1.91/8.29 12.7/1.91/1.59/7.93	105 98 105	5.14 8.86 3.08	3–320 3–320 3–320			Methanol, butanol, water and R113	Offset-strip	Vertical upflow One side electrically heated	100
Mandrusiak et al. [35]	12.7/3.8/1.59/7.93	105	5.14	4–60			Methanol, butanol and water	Offset-strip	Horizontal One side electrically heated	100
Koyama et al. [36]	3.30/6.147/0.203/1.275	677	2.11	28, 55, 70	30, 50		R123	Offset-strip	Vertical downflow One side electrically heated	100
Feldman [37,38]	3.18/6.93/0.2/1.21 (osf1) 9.52/6.93/0.2/1.16 (osf2) −/6.93/0.2/1.21 (perf1) −/3.23/0.2/1.21 (perf2) −/6.93/0.2/0.95 (perf 3)	709 736 709 709 866	2.06 1.985 2.06 1.76 1.68	19–49 19–49 19–49 19–49 19–49	1.4–3.54 1.4–3.54 1.4–3.54 1.4–3.54 1.4–3.54	 1.2–3	R114 R114 R114 R114 R114	Offset-strip Offset-strip Perforated Perforated Perforated	Vertical upflow Both sides electrically heated	300
Watel and Thonon [39]	3.175/6.93/0.2/0.888	919.2	1.574	12–71	0.2–7.4	0.2–2	Propane	Offset-strip	Vertical upflow Fluid (glycoled solution) heated	800

film evaporation of pure refrigerant HCFC123 flowing downward in a vertical rectangular channel with serrated fins. The test section was electrically heated on one side with a transparent plate cover on the other side to observe the flow pattern in the evaporation process directly. They analysed the variation of local convective boiling coefficients with vapour quality, mass flux and heat flux.

In recent years, GREThh (Groupement pour la Recherche sur les Echangeurs Thermiques) has been engaged in research into the compact plate-fin heat exchanger in two-phase applications. In particular, Feldman [37,38] analysed local boiling heat transfer coefficients against vapour quality, deduced from upflow boiling tests of CFC114 in serrated and perforated fin vertical passages of different sizes, sandwiched between electrically heated plates, at a saturation pressure of 0.3 MPa and different heat and mass fluxes.

Watel and Thonon [39] presented local heat transfer results of experiments during boiling of a pure refrigerant (propane) during a vertical upflow inside a compact serrated plate fin exchanger. The heat duty of the heat exchanger to evaporate propane was given by a glycol–water solution, both fluids flowing in counter-current.

2.2. Presentation of experimental studies in small circular and rectangular channels

To understand the heat transfer mechanisms occurring in compact heat exchangers, interesting information can be obtained from the studies on flow boiling in small channels. Most of the studies presented below relate to boiling in individual, small, circular and rectangular channels as a part of a study of compact two-phase heat exchangers, while some other authors [3,8,17] directly used heat exchangers test sections characterised by small multichannel passages operating in parallel (Fig. 1). Channel geometry, test conditions and fluids used in those studies are summarised in Table 2.

Lazarek and Black [40] measured the local boiling heat transfer coefficient, pressure drop and critical heat flux for saturated flow boiling of R113 in an individual 3.15 mm diameter vertical circular tube. The smooth stainless steel tube was uniformly heated by supplying to it direct current electrical power. Inlet subcoolings (differences between the saturation temperature and the fluid temperature at the inlet of the tube) spanned the range 3 to 73 K. They presented their experimental boiling curves and the plot of local boiling heat transfer coefficients as a function of vapour quality and heat flux.

Troniewski and Witczak [41] studied flow boiling of water in individual electrically heated rectangular channels, oriented both vertically and horizontally. They plotted the local boiling heat transfer coefficients against vapour quality, for fixed heat and mass fluxes and against heat flux, for fixed vapour qualities and mass fluxes.

Kenning and Cooper [42] obtained experimental data for upflow boiling of water in individual vertical tubes of 9.6 and 14.4 mm diameters. The test section formed from cupronickel tubing was uniformly heated by current from a DC rotary generator. They reported the local boiling heat transfer coefficients against vapour quality, for fixed heat and mass fluxes.

Moriyama et al. [20] investigated flow pattern, pressure drop and local heat transfer of R113 in saturated flow boiling in single narrow rectangular horizontal channels with width of 30 mm and height in the range 35–110 μm formed between two horizontal parallel plates. The lower and upper walls consisted of respectively a nickel plate and a heater plate uniformly joule-heated. The gap between the plates was adjusted by a spacer made of nickel foil. They presented the local boiling heat transfer coefficients against vapour quality and the boiling curves, for different mass fluxes.

Cornwell and Kew [3] visualised the different flow regimes exhibited by flow in a vertical multichannel heat exchanger in which refrigerant R113 was evaporated and measured mean boiling heat transfer coefficients, for fixed heat and mass fluxes. They reported heat transfer coefficients against heat flux. The test section was representative of a single plate within a compact evaporator. Parallel flow channels were machined into one surface of an aluminium block, electrically heated by five cartridge heaters. A glass plate was clamped over the front surface of the block to allow flow observation.

Peng and Wang [17] experimentally investigated the single-phase forced-flow convection and boiling characteristics of subcooled water flowing through horizontal microchannels operating in parallel with rectangular cross-section 0.6×0.7 mm^2. The liquid subcooling varied from 40 to 70 K. Three parallel identically sized microchannels were machined into the top surface of the stainless steel plate 2 mm thick, being uniformly distributed on the plate. The stainless steel plate was electrically heated by use of an electrical current transformer matched with an SCR voltage regulator, so that reasonably uniform heat fluxes were applied on three sides of each channel. A cover made of Pyrex was fixed on the plate and allowed to observe the flow. The authors inspected the influences of liquid velocity and subcooling on the experimental boiling curves.

Wattelet et al. [11] presented experimental local boiling heat transfer coefficients against vapour quality, for two different refrigerants (HFC-134a and CFC-12) flowing in an individual 10.21 mm diameter horizontal, smooth copper tube for fixed heat and mass fluxes. Heat was applied to the tube using electric resistance heaters wrapped along the tube. Flow patterns during the evaporating process were determined by strobe-light-enhanced visual observation through sight glasses at the inlet and outlet of the test section. Wattelet et al. [14] supplemented the previous work by performing the experiments for the same refrigerants flowing in a 7.04 mm diameter horizontal, smooth copper tube, at lower mass flux conditions.

Tran, Wambsganss and their coworkers studied local flow boiling of different refrigerants in single small rectangular or circular channels. The channel dimensions were representa-

Table 2
Summary of research studies with small circular and rectangular channels

Researcher(s)	Channel size (mm)	D_h (mm)	$\dot{m}$ (kg·m^{-2}·s^{-1})	$\dot{q}$ (kW·m^{-2})	ΔT_{sat} (K)	Fluids	Geometry	Orientation/Heating	p_{sat} (kPa)
Lazarek and Black [40]		3.15	127–750	14–380	3.5–20	R113	Circular Single-channel	Vertical (upflow and downflow) Electrically heated	130–410
Troniewski and Witczak [41]	16.3 × 10.9 21 × 8.5 24 × 7.4	13.1 12.1 11.4	30–160	5–40		Water	Rectangular Single-channel	Vertical and horizontal Electrically heated	100
Kenning and Cooper [42]		9.6 14.4	123–630 55–334	<400 <100		Water	Circular Single-channel	Vertical upflow Electrically heated	160–600
Moriyama et al. [20]	30 × 0.11 30 × 0.035	0.22 0.07	200–1000	4–30		R113	Rectangular Single-channel	Horizontal Upper wall electrically heated	100–200
Cornwell and Kew [3]	1.2 × 0.9 3.25 × 1.1	1.03 1.64	117–627	3–20		R113	Rectangular Multichannel	Vertical upflow Three sides of the channel electrically heated	
Peng and Wang [17]	0.6 × 0.7	0.647	1500–4000	20–1000		Water	Rectangular Multichannel	Horizontal Three sides of the channel electrically heated	100
Wattelet et al. [11]		10.21	100–500	5–30		R12 R134a	Circular Single-channel	Horizontal Electrically heated	363 350
Wattelet et al. [14]		7.04	25–100	2–10		R12 R134a	Circular Single-channel	Horizontal Electrically heated	180–360 165–350
Wambsganss et al. [24]		2.92	50–300	8.8–91	7.2–18.2	R113	Circular Single-channel	Horizontal Electrically heated	124–160
Tran et al. [6]	4.06 × 1.7	2.4	54–396	4–34	1.8–5	R12	Rectangular Single-channel	Horizontal Electrically heated	760–950
Tran et al. [25]	 1.7 × 4.06	2.46 2.4	63–832 44–505	3.6–59.5 5.6–129	1.2–6.6 1.8–8.2	R12 R12	Circular Rectangular Single-channel	Horizontal Electrically heated	510, 820 820
Tran et al. [7]		2.46	92–476	7.9–49.8	2.8–7.1	R134a	Circular Single-channel	Horizontal Electrically heated	400–800
Mertz et al. [8]	1 × 1 1 × 2 1 × 3 2 × 2 2 × 4 3 × 3	1 1.33 1.5 2 2.67 3	50–300 for multichannel test section, 200–700 for single-channel and prototype	3–200		Water and R141b	Multichannel: rectangular Single-channel: rectangular& semi-circular	Vertical upflow Three sides electrically heated	100, 200
Shin et al. [43]		7.7	265–742	10–30		R22, R32, R134a, R290, R600a	Circular Single-channel	Horizontal flow Electrically heated	$T_{sat} = 12\,^{\circ}C$
Kew and Cornwell [9]		1.39–3.69	188–1480	9.7–90		R141b	Circular Single-channel	Horizontal flow, Electrically heated	100
Oh et al. [10]		2 1 0.75	240–720	10–20		R134a	Circular Single-channel	Horizontal flow, Electrically heated	400
Kureta et al. [44]		2 6	100–5000	<2000		Water	Circular Single-channel	Vertical upflow, Electrically heated	100

tive of flow passages in compact heat exchangers. The test channels were uniformly heated by passing electrical current through the channel walls. Wambsganss et al. [24] reported local boiling heat transfer coefficients against vapour quality for R113 flowing in a 2.92 mm diameter stainless steel horizontal tube, for fixed heat and mass fluxes. Tran et al. [6] presented experimental boiling heat transfer coefficients against vapour quality and boiling curves for R12 flowing in a small rectangular horizontal brass channel ($D_h = 2.4$ mm). Tran et al. [7,25] reported local boiling heat transfer coefficients against vapour quality and mass flux as well as boiling curves for R12 and R134a flowing in a small circular channel ($D = 2.46$ mm) and a small rectangular channel ($D_h = 2.4$ mm), both horizontal and fabricated from brass.

Mertz et al. [8] studied flow boiling heat transfer of water and R141b in vertical copper multichannel and single-channel test-sections and an industrial prototype. More precisely, the multichannel test surfaces consisted of planar copper plates with rotary-grinded narrow rectangular parallel channels. These plates were sandwiched between a copper block electrically heated by heater cartridges and a glass plate for observation and photography of the boiling phenomena in the channel test sections. As industrial prototype, a section of a commercial extruded compact heat exchanger was used, made of aluminium with 8 parallel channels. They presented the experimental boiling curves and the average and local heat transfer coefficients against heat flux.

Shin et al. [43] presented experimental data of local convective boiling heat transfer coefficients against vapour quality, for different refrigerants flowing in a single 7.7 mm diameter stainless steel horizontal tube, for fixed heat and mass fluxes. The tube was uniformly heated by applying electric current directly to the tube.

Kew and Cornwell [9] measured pressure drop and local boiling heat transfer coefficients for R141b flowing through narrow horizontal single-tube test sections with diameters of 1.39–3.69 mm. All test sections were thin-walled stainless steel tubes and were heated by passage of a DC electric current along the tube. The test section was enclosed in a 22 mm diameter copper tube which was heated with three independently controlled guard heaters. The authors presented the measured variation in boiling heat transfer coefficient with vapour quality, for fixed heat and mass fluxes. In parallel, they used another flow loop to visualise the adiabatic two-phase upflow within the channels of a vertical multichannel test section either directly through a window or by video or photographic means.

Oh et al. [10] conducted a study for a high efficiency heat exchanger which uses capillary tubes for refrigeration, air-conditioning and heat pump applications. They examined the effects of capillary tube diameters, vapour qualities, heat fluxes and mass fluxes on the measured local heat transfer coefficients and pressure drops of R134a evaporating inside a single capillary horizontal tube. A uniform heat flux on the copper capillary tube was obtained by using a flexible heater wrapped around the outside wall of the tube.

Kureta et al. [44] measured pressure drop and local heat transfer coefficients for boiling two-phase flows of water in single small-diameter vertical tubes at atmospheric pressure, high heat fluxes and inlet water subcooling of 80 K. The test section was joule-heated by a stabilised direct-current electric power supply. By plotting the boiling curves and Nusselt numbers against vapour quality for different tests, they studied the effects of tube diameter, distance from the entrance of the heated section, mass flux and heat flux on subcooled and saturated boiling heat transfer.

2.3. Presentation of experimental studies in confined spaces

Several researches have been carried out on nucleate boiling in confined spaces formed by either annuli or narrow gaps between flat plates. Since nucleate boiling can be a dominant heat transfer mechanism for flow boiling in small channels, useful information about the mechanisms of boiling in compact heat exchanger passages can be obtained from the investigations of nucleate boiling in confined spaces. Therefore, some of them are reviewed below. Channel geometry, test conditions, and fluids used in these studies are summarised in Table 3. In almost all these studies [16,45–49], the flow was induced by natural circulation and the fluid flow velocities were inherently low. Only in the presented study of Aritomi et al. [50], there was a forced flow.

Ishibashi and Nishikawa [45] reported the results of experiments conducted on saturated nucleate boiling of several fluids in various vertical annuli, for different pressures and heat fluxes. They clarified the space restriction effect on the saturated boiling heat transfer phenomena. The cylindrical inner surface made of copper was electrically heated and the outer surface was transparent to allow for visualisation of the boiling process. The upflow was induced by natural convection. They reported the boiling heat transfer coefficients against heat flux and gap size, for various pressures. They also measured bubble emission frequency in the coalesced bubble region.

Jensen et al. [46] determined experimentally the boiling heat transfer characteristics of water and critical heat flux in a restricted annular geometry simulating the annulus formed by tube-baffle assemblies such as those encountered in a shell-and-tube heat exchanger. The test section consisted of an horizontal annular geometry immersed in a pool of saturated water. The inner tube of the annular space was made of stainless steel, 12.7 mm diameter and heated electrically by direct current power conducted through two aluminium bus bars. The baffle was simulated by a square piece of transite, of various thickness and with a hole representing the outer tube drilled in the centre, the size of which depended on the clearance desired between tube and baffle. Eleven annular gaps were tested. Jensen et al. [46] presented the experimental boiling curves, for various gap sizes.

Table 3
Summary of research studies with confined spaces

Researcher(s)	Test section dimensions (mm)	$\dot{m}$ ($kg \cdot m^{-2} \cdot s^{-1}$)	$\dot{q}$ ($kW \cdot m^{-2}$)	Fluids	Orientation/ Heating	p_{sat} (kPa)
Ishibashi and Nishikawa [45]	Annulus; Inner diameter: 50; Annular gap: 0.6–2 (four gaps)		0.8–67.4	Water	Vertical upflow (natural circulation) Inner surface electrically heated	100–1100
	Annulus; Inner diameter: 80; Annular gap: 1–20 (eight gaps)			Water, sodium oleate and saponin aqueous solutions, ethyl alcohol		100
Jensen et al. [46]	Annular geometry Inner diameter: 12.7 Annular gap: 0.076–1.016 (11 gaps)		3–1000	Water	Horizontal annulus Inner surface electrically heated	
Aoki et al. [47]	Annulus; Inner diameter: 42 Annular gap: 0.2–1.5 (six gaps)		4–48	Water	Vertical upflow (natural circulation) Inner surface electrically heated	100
Fujita et al. [48]	Narrow channel between 30 mm wide flat plates; Gap: 0.15, 0.6, 2, 5		5–600	Water	Vertical upflow (natural circulation) One surface electrically heated	100
Xia et al. [16]	Narrow channel between flat plates Gap: 0.8, 1.5, 3, 5, ∞		0.2–300	R113	Vertical upflow (natural circulation) Two vertical parallel plates with symmetric electrical heating	100
Mertz et al. [49]	Narrow channel between 30 mm wide and 120 mm high flat plates; Gap: 1, 2, 3, 4, 5, ∞		20–250 10–100	Water R113	Orientations tested: vertical, horizontal and 45° with heated surface facing upwards One surface electrically heated	100 100
Aritomi et al. [50]	Annulus; Inner diameter: 10 Annular gap: 0.5, 1, 2, 3	30–603	0–100	R113	Vertical upflow (forced flow) Inner surface electrically heated	100

Aoki et al. [47] performed an experimental study on the nucleate pool boiling phenomena within narrow annular gaps using water. The test section consisted of a vertical annular channel whose inner tube was made of stainless steel and heated electrically with a cartridge heater inserted within the tube. The outer tube, made in Pyrex, allowed to observe the drying and wetting process. The gap width between the two tubes was varied between 0.2 and 1.5 mm. The experimental apparatus was mounted in a pool of water. One of the cases they studied is the case in which water could flow by natural circulation through the gap from the bottom to the top. They presented the experimental boiling curves, for various gap sizes.

Fujita et al. [48] investigated nucleate pool boiling heat transfer and critical heat flux for saturated water in a confined narrow space bounded by a vertical copper rectangular heating plate and an opposed unheated parallel rectangular glass plate. The assembly was installed in the middle of an inner boiling vessel. The flow was induced by natural convection. Three different peripheral conditions were tested. The first was an open periphery where four edges of a confined space were open to the bulk liquid. The second was a closed side periphery where both side edges were closed and the top and bottom edges were open. The third was a closed side and bottom periphery where only the top edge was open to the bulk liquid. The heat flux to the heating surface was supplied by conduction through a copper block from electric heaters. Visual observation by still pictures was carried out along with heat transfer measurements. The authors presented the experimental boiling curves, for various combinations of gap size and periphery conditions.

Xia et al. [16] presented experimental data of boiling heat transfer coefficients of saturated R113 in vertical narrow channels. The channels consisted of a pair of flat vertical parallel plates with symmetric electric heating, either both transparent quartz or both porcelain. The porcelain plates were used for the measurement of temperature distribution on the boiling surface. The transparent quartz plates were used for the observation and photography of the flow pattern. The gap size between the heating plates was varied between 0.8 mm and ∞ (pool boiling on a single vertical plate). The test section was installed in the middle of a boiling tank containing the liquid at saturated state. The flow in the channel resulted from natural convection. The authors presented the experimental boiling curves and boiling heat transfer coefficients against gap size, for fixed heat fluxes.

Pool boiling tests were carried out at GRETh (Groupement pour la Recherche sur les Echangeurs Thermiques) [49] for saturated water or R113 in a confined narrow space bounded by a 30 mm wide and 120 mm high heating copper–aluminium–nickel alloy block and an opposed unheated parallel rectangular Lexan plate. The assembly was immersed in a pool of saturated working fluid. The heat flux to the heating surface was supplied by conduction through the alloy block from electric heaters. The parameters investigated were the

orientation of the confined space (vertical, horizontal and 45° with the heated surface facing upwards), the peripheral boundary condition (all four edges open, or side edges closed and top and bottom edges open) and the gap size (1–5 mm and the unconfined space). In addition, in order to gain insight into the flow patterns in the confined space, a high-speed camera was used to obtain flow visualisation data during boiling of R113. The authors presented the experimental boiling curves for both tested fluids, for various combinations of gap size and periphery conditions.

Aritomi et al. [50] investigated the effect of channel gap on the upflow saturated boiling of R113 in various vertical annuli. The inner surface was electrically heated and the outer surface was transparent. They performed steady-state tests with forced flow for controlled inlet fluid temperature, flow rate and heat flux and also performed reflooding tests. They plotted the experimental boiling curves and F parameter against the Lockhart–Martinelli parameter.

3. Flow patterns in small channels

The estimation of flow boiling heat transfer requires a knowledge of the prevailing flow regimes. The flow pattern during vaporisation of a given fluid flowing inside a small heated passage depends on the four main parameters: mass flux $\dot{m}$, heat flux $\dot{q}$, vapour quality x and channel size. The study of two-phase flow has predominantly consisted of flow in medium size circular tubes of diameter larger than 10 mm. Recently the research has expanded to include studies in narrower rectangular or circular channels. The flow regimes present in small channels and the behaviour of a gas–liquid mixture confined to the space in narrow channels differ from those in large channels due to the increased surface forces and frictional pressure drop. Numerous authors [37] (Table 1), [9] (Table 2), [19,22,51–57] determined by visual observation flow patterns during adiabatic flow of a gas–liquid mixture (air/water mixture most of the time) in small horizontal channels or small vertical channels with upwards gas–liquid two-phase flow. Some of them presented flow regime maps in terms of liquid and vapour superficial velocities independent of heat flux (since their tests were adiabatic). Other investigators [1,2] (Table 1), [3,8,11,14,20] (Table 2), [16,45] (Table 3), [58] observed the successive flows obtained during flow boiling in heated channels for imposed channel size, heat and mass fluxes.

3.1. Sequence of flow patterns with increasing vapour quality

In general, the flow pattern configurations susceptible to be observed successively during upflow boiling in small vertical heated channels with increasing vapour quality are given as follows.

Isolated bubbles flow (typical of nucleate boiling). This flow is characterised by a distribution of small discrete vapour bubbles in a continuous flowing liquid phase, those bubbles detaching from the nucleation sites on the heated surface [19].

Confined bubble flow. In a narrow space, this flow is characterised by generated vapour bubbles coalescing and filling the cross section of the flow channel, leaving a thin liquid film between the vapour bubbles and the heated channel walls [3,9] (Table 2), [45,47,48] (Table 3), [58,59]. The heat transfer surface is washed either by a thin liquid film or a liquid plug [16] (Table 3). The layer of liquid evaporates and causes the bubbles to grow exponentially [9] (Table 2). The coalesced bubbles may be formed by isolated bubbles growing or coalescing, alternatively single bubbles may reach a sufficient size to be regarded as confined as they fill up the narrow space, before becoming detached from their nucleation sites. According to Ishibashi and Nishikawa [45], for nucleate boiling in narrow vertical annuli (Table 3), the confined bubbles departed and rose regularly at a low frequency from the heating surface. These coalesced bubbles were regularly generated one after another in the space, under a slow cycle. They established that coalesced bubble emission frequency N was proportional to $\dot{q}s^{-3/2}$. Monde [60] found the thickness of the thin liquid film between the vapour bubbles and the heated wall was in the range of 60–80 μm and independent of the bubble length. According to Moriyama et al. [20] for flow boiling in extremely narrow channels (Table 2), when the sizes of the bubble are much larger than the thickness of the channel as in their study, the bubble surface forms an extremely small meniscus at the edge, and in such a case, it is expected that the thickness of the liquid film remaining on the wall under the bubble is controlled by a capillary number $Ca = \mu_L \dot{m}(x/\rho_V + (1-x)/\rho_L)/\sigma$.

Slug flow. This flow is obtained when the vapour bubbles diameter tends towards the channel hydraulic diameter. Slug flow then consists of these pockets of gas (commonly called plugs or Taylor bubbles) separated by liquid slugs, both flowing upwards. Each plug of gas contains a half circle cap head and a flat rectangular body and is surrounded by a thin liquid film which flows vertically downwards [19,57]. Some authors [22] do not make the distinction between the confined and slug flow regimes.

Churn flow. This flow is formed by the breakdown of the large gas bubbles in slug flow [57]. The gas flows in a more chaotic manner through the liquid which is mainly displaced to the channel wall.

Annular-slug flow. As the confined bubbles expand [9] (Table 2), liquid in the slugs between them is deposited on the channel wall and the flow becomes basically annular with random irregular slugs of liquid interspersed with the vapour.

Annular flow. This flow is comprised of a solid gaseous core, continuous in the axial direction, with a liquid film surrounding the core, both flowing upwards. The annular flow occurs for the higher vapour qualities or mass fluxes.

Dryout. In the annular flow regime as the liquid film thickness reduces with increasing vapour quality, there is a tendency for the film to break up and partial dryout to occur.

In reality, the observed flow pattern for given vapour quality can vary according to the mass flux, heat flux, channel dimensions, fin geometry, orientation and pressure.

3.2. Effect of mass flux

The various flow regime maps proposed by different authors easily show that for given channel dimensions, fluid and vapour quality, the regime of flow depends on mass flux. For example, Cornwell and Kew [3] noticed that during flow boiling in a small vertical channel (Table 2), at low mass flow rates and low vapour quality, confined bubbles which straddled the channel might occur while at higher flow rates, isolated bubbles might occur at the same position and quality. At low flow rates, bubbles might grow to fill the channel at the nucleation site, thus precluding the isolated bubbles regime. It is deduced from several experimental studies [2,36] (Table 1), [10,11] (Table 2) that the lower the mass flux, the slightly lower vapour quality at which the transition between annular flow and dryout region begins.

3.3. Effect of heat flux

Several authors [8] (Table 2), [45,47] (Table 3) underlined that the frequencies of bubble generation increased with heat flux. For example, in the experimental study of nucleate boiling in narrow vertical annuli, Aoki et al. [47] underlined that for gap width $s = 1$ mm, the bubbles generated on the heating inner surface were pressed by the outer tube and grew in flattened shapes covering the heating surface, and then flowed out from the top end, forcing the liquid upwards. With an increase in heat flux, the density of bubble generation increased and the bubbles coalesced and grew, changing shape randomly. As the heat flux became higher, the gap was occupied by a great number of bubbles and liquid penetrated into the gap as scattering droplets, with repeated local drying and wetting. For the case of the gap width of 0.2 mm and low heat flux, comparatively small bubbles were generated and rose as if by crawling within the gap. With an increase in the heat flux, the alternatively drying and wetting areas grew in extent and finally the heating surface became completely dry except for the top and bottom ends. In fact, in the isolated or confined bubbles region, for large enough heat fluxes applied on the channel wall, the wall dries out. The heat flux at which this dryout occurs is called critical heat flux CHF. Intermittent local dryout may also occur in the confined bubble regime, in confined tubes or narrow annuli at low vapour quality and moderate heat flux prior to critical heat flux if areas of the liquid film deposited beneath the confined bubbles evaporate fully before being replenished, which has been observed by various authors [9] (Table 2), [45,47] (Table 3), [61]. Lazarek and Black [40] (Table 2) developed a new correlation which predicts the vapour quality for the onset of critical heat flux. This critical vapour quality decreases with the increase in mass flux or tube diameter.

Several researchers [2,36] (Table 1), [10,11] (Table 2) obtained that the transition from annular flow to dryout began at lower qualities when increasing the heat flux. For example, according to Wattelet et al. [11], for flow boiling in an horizontal tube, dryout began to occur between 55 and 70% quality for the 20 and 30 $kW{\cdot}m^{-2}$ cases and between 75 and 85 % for 5 and 10 $kW{\cdot}m^{-2}$, respectively.

3.4. Effect of channel dimensions

The passage dimensions also have an important effect on the observed flow patterns.

3.4.1. Effect on the observed flow in the nucleate boiling region

For test conditions corresponding to nucleate boiling dominance, whereas isolated bubbles are observed in large channels, a confined bubbles or slug flow regime is more usually observed in small channels. In particular, several investigators [3] (Table 2), [16,45,47,48] (Table 3), [58] have shown that, in the nucleate boiling region, when the gap size is larger than a critical value depending on pressure and fluid, the bubbles generated in the channel will not be deformed and the boiling flow pattern is similar to that of nucleate boiling in tubes with larger diameters. At the opposite, as the gap size decreases below the critical value, coalesced (confined) bubbles are generated instead of isolated bubbles. Whereas a classical ebullition cycle includes nucleation, bubble growth, departure and rise, when the boiling space is small relative to bubble sizes, growth and departure of the coalesced bubbles are affected by the channel walls. For example, bubbles will be squeezed by the walls and flatten out. Bubble diameters become so large that adjacent bubbles coalesce.

Several authors determined the channel critical size defining the transition between the isolated bubble regime and the confined bubble regime. For example, for water nucleate boiling at atmospheric pressure in various annuli, Ishibashi and Nishikawa [45] (Table 3) noted that at the clearance of 3 mm or more, small isolated bubbles of diameters between 3 and 3.5 mm were generated from the heating surface. When the space dimension was reduced to less than 3 mm, only coalesced bubbles were generated. According to Xia et al. [16] (Table 3), for nucleate boiling of R113 at atmospheric pressure in a narrow vertical channel, for high heat fluxes, when gap size was 3 mm or larger, isolated bubbles were generated from the boiling surface. When gap size was smaller than 3 mm, the generation of few isolated bub-

bles could be observed, but large squeezed coalesced bubbles were generated in the channels. Cornwell and Kew [3] (Table 2), [58] suggested to use the Confinement number, which represents the ratio of a characteristic bubble departure size and the mean hydraulic diameter of the flow channel, $Co = [\sigma/\{g(\rho_L - \rho_V)\}]^{0.5}/D_h$ for evaluating the transition between the isolated bubble regime and the confined bubble regime. For $Co > 0.5$, the flow pattern is typically "confined" and for $Co < 0.5$, isolated bubbles are present. Co increases when the channel dimension is reduced.

3.4.2. Effect on vapour quality at transition from bubbly to slug, slug to churn and churn to annular flow

The vapour qualities at which transitions between the flow regimes occur depend on the channel dimensions and orientation. For example, in experimental studies on adiabatic air–water two-phase flow regimes in vertical rectangular channels with mini gaps or small diameter tubes [19,22, 57], transition from bubbly to slug, slug to churn and churn to annular flow occurs at lower superficial gas velocities (i.e., lower vapour qualities) in the smaller channels/tubes. According to Xu [57], the bubbly to slug flow transition appears at lower superficial gas velocity in the channel with the gap of 0.6 mm than that with the gap of 1 mm because the distances between the neighbouring bubbles are decreased to induce the small bubbles merging. Moreover, the transition lines from slug to churn flow and from churn to annular flow occur at lower gas flow rate in the smaller channels due to the increased wall and interface shear stresses. Furthermore, in the channel with the gap of 0.3 mm or less, Xu [57] noted that bubbly flow was never observed. Instead, the small bubbles were squeezed forming a cap-bubbly flow. For flow boiling in small rectangular channels, at low flow rate, Mertz et al. [8] (Table 2) concluded that bubbles might grow to fill the channel at the nucleation site, the bubble generation rate was increased and it was impossible to observe single vapour bubbles and the flow configurations observed successively with increasing vapour quality were confined bubbles or slug flow and annular flow.

Lin et al. [22] concluded that existing flow maps could predict flow regimes, however the observed flow regime boundaries were dependent on size and geometry of flow passages and experimental conditions. At the opposite of studies in vertical channels, in experimental studies on adiabatic air–water two-phase flow regimes in small horizontal rectangular or circular channels [52,54], transition from intermittent flow (covering slug, plug and churn flow) to annular flow occurs at larger superficial gas velocity (i.e., higher vapour quality) when the channel dimensions are reduced. Wambsganss et al. [24] (Table 2) showed that the small-diameter horizontal channels produced a slug flow pattern over a large range of parameters when compared with larger-diameter channels. According to them, the slug flow enabled boiling to be maintained at higher qualities than in larger tubes, the annular flow generally did not start until qualities of 0.6 to 0.8. They stated that for larger channel sizes, annular flow prevailed up to the critical heat flux, whereas for smaller channels, the crest of a wave on a liquid film was able to reach the opposite wall producing a slug of liquid in a situation that would have normally produced annular flow in a larger channel. As for vertical channels, Wambsganss et al. [54] concluded that when channel dimensions were too small, the isolated bubble flow was no more observed.

Concerning the effect of channel dimensions on transition to dryout, the conclusions are opposite according to different authors. Indeed, whereas in Oh et al.'s study [10] about flow boiling in an horizontal tube (Table 2), the vapour quality where the heated wall dried out decreased with decreasing channel dimensions, on the contrary, in Moriyama et al.'s study [20] on flow boiling in an horizontal rectangular channel (Table 2), it slightly increased with decreasing gap size.

3.5. Effect of fin geometry in compact plate-fin heat exchangers

According to Carey [5], in serrated or perforated-fin passages, unlike round vertical tubes, the two-phase transport is usually non-uniform over the perimeter of the passage at any downstream location. This results from the effect of the irregularity of the passage on the two-phase flow and from the configuration of the compact heat exchanger which causes the thermal boundary condition to be non-uniform over the passage wall. At high quality in serrated fin passages (Fig. 2), liquid flowing in a film along fins may be shed from the trailing edges of these fins into the core flow. Alternatively, always when the liquid film reaches the trailing edge of the fin, at locations near the prime surface walls, surface tension may force the liquid on the fin to merge into the liquid films on the prime surface walls. In offset fin surfaces, liquid is delivered to the fins by two mechanisms: entrained liquid droplets may be deposited on the fin surfaces, and liquid from the prime surface walls may be dragged onto the fins by lateral Reynolds stresses exerted by the turbulent core flow on the prime-surface liquid film. The efficiency of convective vaporisation processes in such passages will depend directly on how effectively liquid can be delivered to surfaces of fin structures downstream of the location where shedding occurs.

3.6. Effect of gravity (orientation)

Gravity effects, resulting from channel orientation, are important in phase-change heat transfer in large enough channels because they can influence flow patterns. Especially, various authors [14] (Table 2), [52,62–64] noticed that in horizontal flow, there was a loss of wetting for low mass fluxes and the flow was wavy-stratified, i.e., liquid flowed along the bottom of the channel as gravity forces dominated, whereas for higher mass fluxes, higher vapour qualities, the flow would have been annular, as in vertical flow. According to Wattelet et al. [11], for flow boiling in an horizontal tube

(Table 2), in the dryout region, the annular flow was intermittently present with the dryout occurring in an oscillatory pattern. Indeed, in horizontal tubes with uniform heat flux, dryout first occurs in the top region of the tube where the liquid layer is thinner.

In small channels, it is generally reasoned that gravity effects are of less importance because surface tension forces dominate gravity forces. The gravity does not exert any influence on the flow pattern inside tubes and the liquid film thickness is almost uniform in the circumferential direction due to the surface tension force having more and more significant influence when the tube diameter becomes smaller and smaller. For example, Damianides and Westwater [52] experimentally determined the flow maps for air–water mixtures in an horizontal offset-fin compact heat-exchanger and in horizontal glass tubes of 1 to 5 mm diameter. They underlined the absence of stratified flow in the compact heat exchanger and the tube of 1 mm diameter, whereas the stratified wavy regime was observed in the tubes of 2 to 5 mm diameter. Instead of the stratified flow in the smaller tubes, an important portion of the map area was covered by the intermittent regimes (plug, slug and churn flows).

3.7. Effect of pressure

Ishibashi and Nishikawa [45], who studied nucleate boiling of several fluids in various vertical annuli (Table 3) deduced that in the coalesced-bubble region, when the pressure was increased sufficiently, a pressure was reached at which coalesced bubbles were not seen and isolated bubbles were generated. They explained these trends by the fact that the higher the pressure was, the more the coalesced bubble emission frequency was reduced.

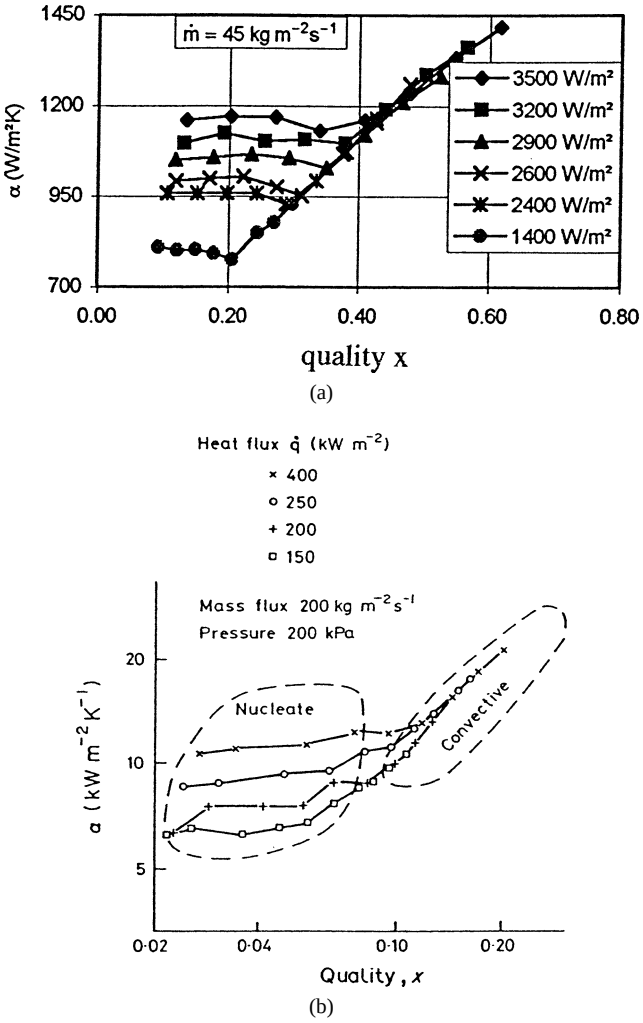

Fig. 3. (a) Feldman [37,38] data (Table 1, perf3), (b) Cooper [68], Kenning and Cooper [42] data (Table 2, 9.6 mm diameter tube).

4. Typical trends of heat transfer coefficient in the two regions of boiling

It is now well known that boiling heat transfer for flow inside channels is governed by two mechanisms: nucleate boiling and convective boiling. Nucleate boiling is characterised by the formation of vapour bubbles at a heated wall when nucleation conditions, i.e., a thin liquid layer near the surface superheated enough to allow nucleation, are reached. Convective boiling is characterised by heat transferred by conduction and convection through the liquid film and vaporisation at the liquid/vapour interface. Through representation of heat transfer coefficient against vapour quality, mass or heat flux, it is possible to identify the two regions of boiling and the heat transfer trends in each region. The flow boiling heat transfer coefficient is defined as:

$$\alpha = \dot{q}/\Delta T_{\text{sat}} \tag{1}$$

In several experimental studies on flow boiling in large tubes [65–67] and in smaller passages [37,38] (Table 1), [9, 10,14,25,41–43] (Table 2), [68], the obtained heat transfer data cover the two boiling regions. For example, Fig. 3(a) shows the experimental data of Feldman [37,38] (Table 1); Fig. 3(b) shows the data of Kenning and Cooper [42] (Table 2) and Cooper [68]. Basing on numerous authors' results, the typical trends of the heat transfer coefficient obtained against vapour quality, for given mass and heat fluxes, are shown in Fig. 4(a), in case the flow associated to convective boiling is the annular flow. The deduced heat transfer coefficients against mass flux, for given vapour qualities and heat fluxes, and against heat flux, for given vapour qualities and mass fluxes, are shown in Fig. 4(b) and (c) respectively. Some authors [4,12] (Table 1), [25] (Table 2), [66] used the boiling curve (log–log plot of heat flux against wall superheat) illustrated in Fig. 5 as a tool to distinguish between the two dominant mechanisms of flow boiling. These figures show the heat transfer characteristics in the two regions of vaporisation.

In nucleate-dominated flow boiling, the heat transfer coefficient called α_{nb}, is independent of mass flux and

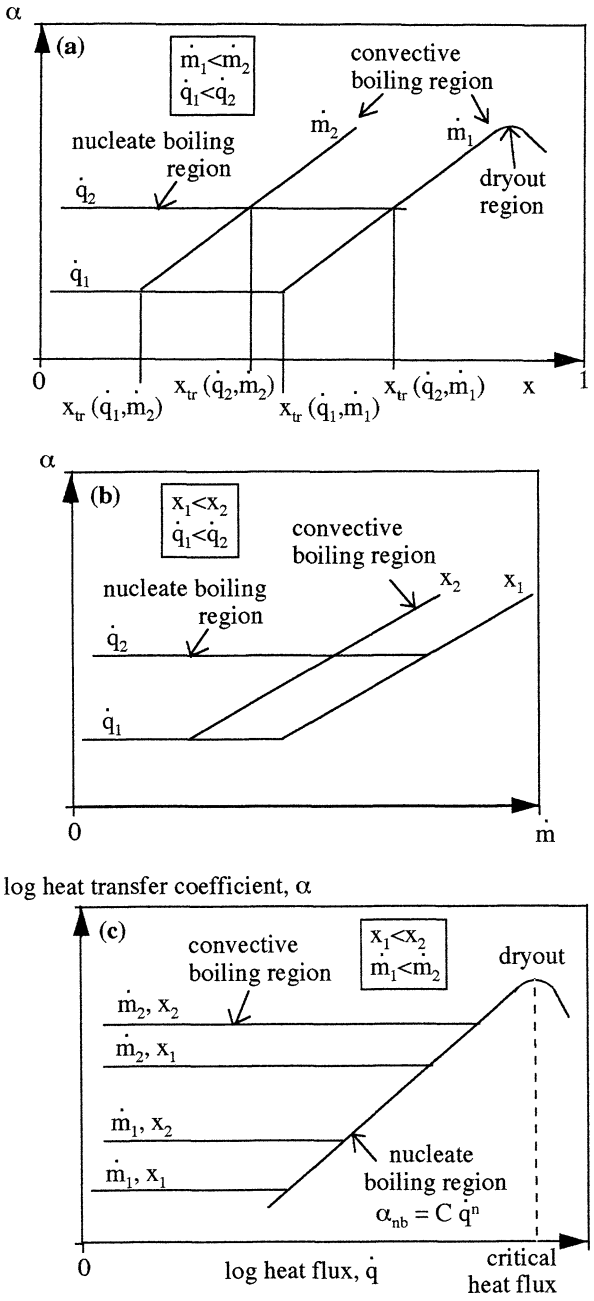

Fig. 4. Heat transfer coefficient trends against (a) vapour quality, (b) mass flux, (c) heat flux. Trends deduced basing on [9,10,14,25,37,38,41–43,65, 67,68].

vapour quality, increases with increasing heat flux (or wall superheat), and is sensitive to saturation pressure level (the heat transfer coefficient increases as pressure increases). In Figs. 4(c) and 5, these data will define single straight lines with a slope respectively lower and greater than unity. This observation suggests that a power function relationship exists between heat transfer coefficient and heat flux as well as between heat flux and wall superheat. These relationships are developed in Section 6.2.

On the other hand, in convective-dominated flow boiling (when nucleate boiling appears to be largely suppressed),

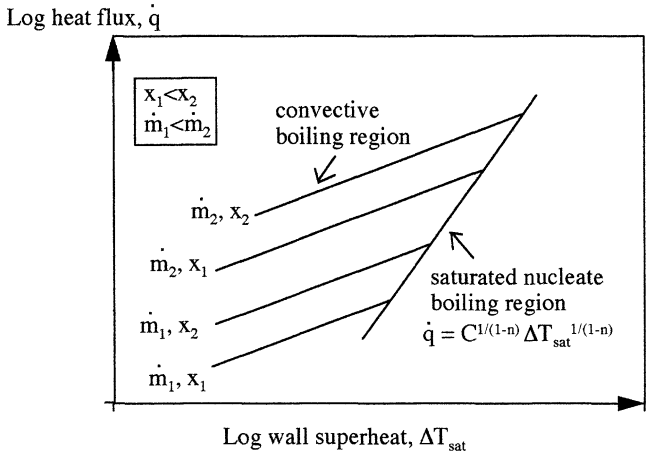

Fig. 5. Boiling curve.

the heat transfer coefficient called α_{cv}, is independent of heat flux (or wall superheat) and increases with increasing mass flux and vapour quality. Therefore, for given vapour quality and mass flux, the resulting boiling curves of heat flux versus wall superheat will be straight lines with slopes approximately equal to unity. In this region, the wall superheats are too low to sustain nucleate boiling. The increase in the heat transfer coefficient with increasing vapour quality in the convective boiling region is due to the parallel decrease in the liquid film thickness and an increased velocity of the vapour phase [43] (Table 2). Intense evaporation at the liquid-vapour interface diminishes the liquid film thickness, reducing the thermal resistance associated with the heat conduction across the film and increasing the heat transfer coefficient [11,14] (Table 2). Thus, at high vapour qualities, nucleate boiling is suppressed due to significant cooling promoted by the thinning of the annular flow.

Moreover, in the convective boiling region, for vapour quality higher than a value depending on test conditions, some authors [2,36] (Table 1), [9–11,20,43] (Table 2) observed a decrease of heat transfer coefficient supposed to be caused by the emergence of the post dryout region through the disappearance of the liquid film covering the tube wall. The heat transfer coefficient falls toward the value of gas single-phase flow (Fig. 4(a)).

Even in the nucleate boiling region, for large enough heat fluxes applied on the channel wall, dryout of the wall occurs which causes a marked decrease in the heat transfer coefficient (Fig. 4(c)) and an increase in the heating surface temperature [16,45,47,48] (Table 3). The heat flux at which this dryout occurs is called the critical heat flux.

In general, convective boiling dominates for low values of heat flux and wall superheat and high vapour qualities, and nucleate boiling dominates for high values of heat flux and wall superheat and for the lower vapour qualities. There exist numerous experimental studies on flow boiling in small passages where the heat transfer data belong to only one of the two boiling regions, either nucleate boiling or forced con-

vective boiling region. In particular, in experiments on small single, smooth (circular and rectangular) channels (hydraulic diameter approximately 2.5–3 mm) or narrow spaces, the major part of the results of more or less recent researches [6, 17,24,25,40,41] (Table 2), [16,45,50] (Table 3), [26,27,29, 30] provided evidence that for high heat fluxes and high superheats and low mass fluxes (<300 kg·m^{-2}·s^{-1}), a nucleation mechanism dominated up to high mass qualities (80%). The results provided a clear indication that the heat transfer coefficient was a strong function of heat flux and only weakly dependent on mass flux and vapour quality. On the other hand, for the studies of Robertson, Wadekar and coworkers at HTFS [4,12,13,32–34] (Table 1) on flow boiling in perforated and offset-strip fin passages, the tests were performed within the range of operational parameters encountered in industrial cryogenic applications, at low values of heat flux (<4 kW·m^{-2}) and wall superheat (<2.5 K). The base wall superheat was sufficiently low that nucleate boiling effects were negligible and the dominant mechanism of heat transfer was convective boiling; the results provided a clear indication that the heat transfer coefficient was independent of heat flux, dependent on mass flux and generally increases with increasing vapour quality. For the range of test conditions of several other authors [1,2] (except at low qualities with some tests), [39] (Table 1), [11,20] (Table 2), nucleate boiling was also suppressed.

The mechanism of the transition between the two regimes can be abrupt or more gradual. Correlations for flow boiling in conventionally-sized heat exchangers have usually been based on nucleate and convective boiling components of the heat transfer coefficient, α_{nb} and α_{cv}, respectively. These components are superimposed by a very complex mechanism. Three main models exist in present literature [67], the "superposition", "asymptotic" and "enhancement" models. The superposition model uses addition of the two components with a suppression factor S [65]:

$$\alpha = S\alpha_{nb} + \alpha_{cv} \tag{2}$$

The suppression factor was used by Chen [65] in order to take the suppression of nucleate boiling with the increase in flow velocity into account. He correlated the S factor as a function of the two-phase Reynolds number $Re_{TP} = (\alpha/\alpha_L)^{1.25} Re_L$.

The enhancement model was proposed by Shah [62] for flow in tubes. For flow in vertical tubes, it is described by:

$$\alpha = E\alpha_L \tag{3}$$

where E is the "enhancement factor", which is a function of the boiling number (Bo) and the convection number (Co_{Shah}).

The asymptotic model used by various authors [25,37, 38,41–43,66,67] is based on asymptotic addition of the two boiling components:

$$\alpha^m = \alpha_{nb}^m + \alpha_{cv}^m \tag{4}$$

In Eq. (4), the m value assures a more or less abrupt transition between the nucleate and convective boiling regions. The case $m = 1$ represents the superposition model; $m \to \infty$ is the case for which the larger of the two mechanisms is predominant, the other contribution being negligible, i.e., the heat transfer coefficient is equal to the larger of convective coefficient α_{cv} or nucleate boiling coefficient α_{nb}. According to the results obtained in previous studies [37,38] (Table 1), [14,25,41–43] (Table 2), [66,67], the analysis of the heat transfer mechanisms in small passages showed that the transition between the two boiling regions was rather abrupt. It is deduced that the asymptotic model with high values of m (from 2.5 in [14] to ∞ in [37,38,42]) is the mostly adapted to flow boiling in small passages. Thus, vapour quality x_{tr} at which the transition between nucleate and convective boiling occurs, for given mass and heat fluxes, can be determined precisely. In the representation of the heat transfer coefficient given in Fig. 4(a), it can be observed that x_{tr} increases with the heat flux, at a given mass flux and decreases with increasing mass flux, at a given heat flux.

It is deduced from Fig. 5 that the wall superheat associated with the transition from convective to nucleate boiling region increases with mass flux and vapour quality. It is also recognised to be a function of the fluid and the channel (geometry, size and surface condition). For example, the transition between regions of convection and nucleation dominance occurs at a lower wall superheat as channel size decreases [6,7,25] (Table 2). More precisely, for the previous authors' tests, this transition occurred at a low wall superheat of approximately 3 K (corresponding to a heat flux of 7 kW·m^{-2}) for mass fluxes between 70 and 150 kg·m^{-2}·s^{-1}. In the experimental study of Feldman [37,38] (Table 1), the transition wall superheat remained between 1.6 (corresponding to heat flux $\dot{q}$ of 1450 W·m^{-2}) and 2.9 K (corresponding to heat flux $\dot{q}$ of 3540 W·m^{-2}), for mass fluxes between 19 and 49 kg·m^{-2}·s^{-1}. For the same tests, transition vapour quality x_{tr} varied from 0.24 to 0.55. These low transition wall superheats probably stem from the fact that as detailed in Section 6.1, in the nucleate boiling region, the heat transfer coefficient increases with the reduction of gap size. Thus, the contribution of nucleation in heat transfer is more important in small channels as compared with larger ones.

5. Characteristics of convective boiling in small channels

When the predominant heat transfer mechanism is forced convective boiling (where heat transfer is primarily a function of mass flux and vapour quality), the associated flow pattern derived according to previous studies in vertical channels [1,2,4,12,13,32,34,37] (Table 1) is either the intermittent flow including the slug and churn flows at low mass fluxes and low vapour qualities and the non-intermittent flow including the annular flow at higher mass fluxes or vapour qualities. More precisely, in the slug flow region, according to Robertson and Clarke [32], in boiling heat transfer with vertical slug-upflow and with no nucleate boiling present,

there will be two simultaneous mechanisms occurring in parallel: evaporation of the falling liquid film surrounding each rising bubble and sensible heating of the climbing liquid slugs. For horizontal flows, one more flow pattern, the stratified or wavy-stratified flow, can be observed depending on test conditions. For example, according to Wattelet et al. [11, 14] (Table 2), for flow boiling in an horizontal tube, the observed flow is either the wavy-stratified flow at lower mass fluxes and qualities or the annular and misty-annular flow at higher mass fluxes and qualities.

5.1. Effect of vapour quality and mass flux on heat transfer characteristics and associated flow patterns

In order to illustrate the separate effects of vapour quality and mass flux on boiling heat transfer in the intermittent and non-intermittent regions, Robertson, Wadekar and their coworkers [12,13,31–34] (Table 1), and other authors [36] (Table 1), [10,20,42] (Table 2), proposed several types of representation of their experimental data. Either they plotted their measured convective boiling coefficients against Re_{TL}, for various vapour qualities, or they plotted them against vapour quality, for various mass fluxes. Another interesting representation was used by several authors [2,4,34,36] (Table 1), [10,20,42] (Table 2), [69,70] plotting enhancement factor F against $1/X$, the reciprocal of the Martinelli parameter. The following formulation:

$$\alpha_{\mathrm{cv}} = F\alpha_L \tag{5}$$

to express the convective boiling heat transfer coefficient, was first proposed by Chen [65]. Heat transfer coefficient α_L for the liquid phase flowing alone is estimated using a single-phase correlation of the following form:

$$Nu_L = A\,Re_L^a\,Pr_L^b \tag{6}$$

where $Re_L = \dot{m}(1-x)D_h/\mu_L$ and A, a and b are constant which depend on the geometry of channels and nature of the flow. Martinelli parameter X is the square root of the ratio of single phase liquid fraction pressure gradient to the single phase gas fraction pressure gradient:

$$X = \left(\frac{\Delta p_{F,L}}{\Delta p_{F,V}}\right)^{0.5} = \left(\frac{1-x}{x}\right)\left(\frac{f_L\rho_V}{f_V\rho_L}\right)^{0.5} \tag{7}$$

where f_L and f_V are the Fanning friction factors for liquid phase and vapour phase respectively flowing alone. In single-phase flow, friction factors can be expressed by correlations of the following form:

$$f = D\,Re^{-d} \tag{8}$$

where D and d are constants which depend on the geometry of channels and nature of the flow. Thus, f_L and f_V are estimated by using Re_L and Re_V respectively instead of Re in Eq. (8). The Martinelli parameter X is noted X_{tt} for the particular case where liquid and vapour phases are turbulent.

The general convective boiling heat transfer trends in the slug and annular flow regions on perforated fin test sections or small plain channels are given in Figs. 6(a), 7(a) and 8(a) for different mass fluxes ($\dot{m}_1 < \dot{m}_2 < \dot{m}_3 < \dot{m}_4 < \dot{m}_5$). Respective trends on serrated fin test sections are given in Figs. 6(b), 7(b) and 8(b). Those trends have been deduced from a detailed analysis of experimental heat transfer characteristics obtained by different authors, [4,31,32,34] (Table 1), [10,20,42] (Table 2), [69–71] on perforated fin test sections or small plain channels, [1,2,12,13,33,36] (Table 1) on serrated fin test sections. For example, the experimental heat transfer data obtained by some of the previously cited authors on perforated fin test sections are shown in Figs. 9(a), (b) and (c), in terms of α over x [34], α over Re_{TL} [32] and F over $1/X_{\mathrm{tt}}$ [34], respectively. The characteristics obtained by some other authors on serrated fin test sections are shown in Fig. 10(a), (b) and (c), in terms of α over x [13,33], α over $\dot{m}$ [12] and F over $1/X_{\mathrm{tt}}$ [36], respectively. Robertson, Wadekar and their coworkers used a flow transition criterion, the modified Froude number defined by $j_V^* = \dot{m}x\rho_V^{-1/2}[gD_h(\rho_L-\rho_V)]^{-1/2}$ to distinguish slug/churn flow data from the data in the annular (laminar or turbulent) flow region. The criterion $j_V^* = 1$ defined the transition from slug/churn to annular flow and the data for which the following approximate criterion: $j_V^* < 1$ is satisfied was grouped as slug/churn flow data. j_V^* reflects the ratio of inertia to buoyancy forces in slug flow. The criterion defining the churn/slug-annular flow transition was deduced by McQuillan and Whalley [72]. According to equality $j_V^* = 1$, the range of vapour qualities over which this form of slug flow is maintained is all the more spread out when the fluid mass flux is low. The transition points $(1,\ldots,5)$ for each mass flux and two-phase flow patterns expected to be present in each region are delineated in Figs. 6, 7 and 8. In fact, the value of j_V^* at the transition between the annular and churn/slug regions is not systematically equal to unity, but varies according to the different experimental studies. For example, Carey and Mandrusiak [1] observed for flow boiling in vertical channels with offset strip fins (Table 1) that the transition conditions corresponded approximately to $j_V^* = 0.5$. Kenning and Cooper [42] (Table 2) also deduced that for the 14.4 mm bore tube, the churn-annular flow transition was obtained for $j_V^* = 1$, whereas for the 9.6 mm tube, the annular flow was maintained down to $j_V^* = 0.4$, showing that the criterion does not properly represent the effect of tube diameter. As shown in Fig. 7, mass fluxes $\dot{m}_1$ and $\dot{m}_2$ belong to the region in which the all liquid flow is laminar ($Re_{TL} < Re_{TL,\mathrm{cr}}$) and mass fluxes $\dot{m}_3$, $\dot{m}_4$ and $\dot{m}_5$ belong to the region in which the all liquid flow is turbulent ($Re_{TL} > Re_{TL,\mathrm{cr}}$).

5.1.1. Analysis in slug flow region

The trends of the boiling heat transfer coefficients obtained in the slug flow region, corresponding to $j_V^* < 1$, are shown in Figs. 6, 7 and 8. In forced convective boiling, Robertson and coworkers [12,13,32–34] for the serrated or perforated-fin test section (Table 1), Watel and Thonon [39] for a serrated-fin heat-exchanger (Table 1), Moriyama et

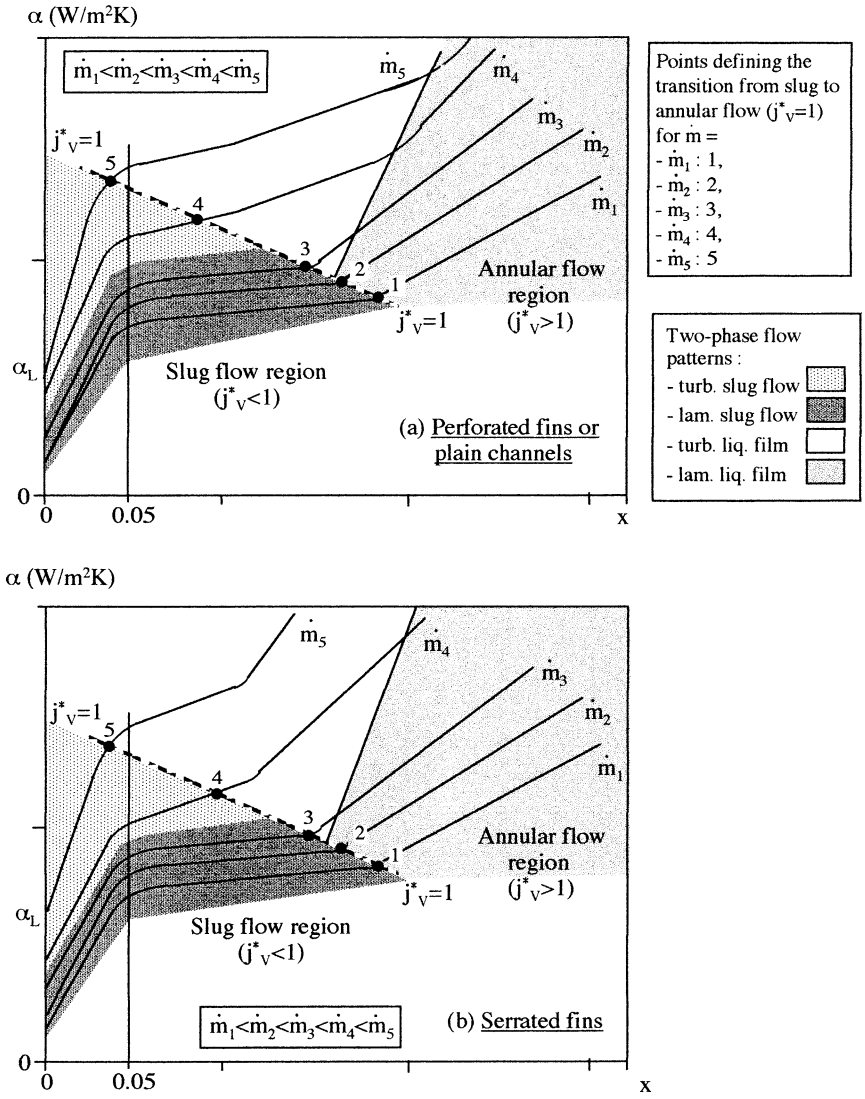

Fig. 6. Main convective boiling heat transfer trends obtained in the slug and annular flow regions against vapour quality. Trends deduced basing in part on: (a) [10,34,42,69,71], (b) [1,2,12,13,33,36].

al. [20] for a narrow channel (Table 2), observed that, at vapour qualities even as low as 0.05, the convective boiling coefficients were considerably greater than the equivalent liquid coefficients, showing the enormous effect of vapour volume on coefficients at very low qualities (Figs. 6 and 7). Moreover, for vapour quality higher than approximately 5%, for a fixed mass flux, the boiling heat transfer coefficient appears to increase very slowly with increasing vapour quality (Fig. 6). For a fixed vapour quality, it increases with increasing mass flux, very slowly for the lower mass fluxes ($\dot{m}_1$, $\dot{m}_2$ and $\dot{m}_3$) in the laminar slug flow region and more rapidly for higher mass fluxes ($\dot{m}_4$) in the turbulent slug flow region (Fig. 7). According to several authors [32,34] (Table 1), [20] (Table 2), in general the low Reynolds numbers due to the small channel dimensions ensure that the heat transfer characteristics of the slug flow pattern are dominated by laminar flow. Robertson [12] correlated his data obtained with nitrogen on a serrated-fin test section (Table 1) for a slug flow in a laminar regime by: $\alpha = 1650 + 1000x$ W·m^{-2}·K^{-1} and a slug flow in a turbulent regime by: $\alpha = \dot{m}^{0.8}(160x + 66)$ W·m^{-2}·K^{-1}. In fact, in the turbulent slug flow region (for example, at $\dot{m}_4$ for the lower qualities), the variation of heat transfer coefficient with mass flux and vapour quality is similar to that in the turbulent liquid film flow region (Fig. 7). In the representation of the heat transfer trends in terms of F and $1/X$ in Fig. 8, in the laminar slug flow region ($j_V^* < 1$), for given mass flux $\dot{m}_1$, $\dot{m}_2$ or $\dot{m}_3$, F increases slowly with increasing $1/X$ (i.e., vapour quality). At a given X value, F decreases with increasing mass flux, except for the perforated fins (Fig. 8(a)) for mass fluxes $\dot{m}_1$ and $\dot{m}_2$ corresponding to laminar liquid fraction heat transfer coefficient α_L. For the other cases, the decrease of F with increasing mass flux is explained by the fact that the magnitude of the increase in the two-phase heat transfer coefficient with increase in mass flux is less than the corresponding increase in the liquid fraction coefficient. Nevertheless, in the perfo-

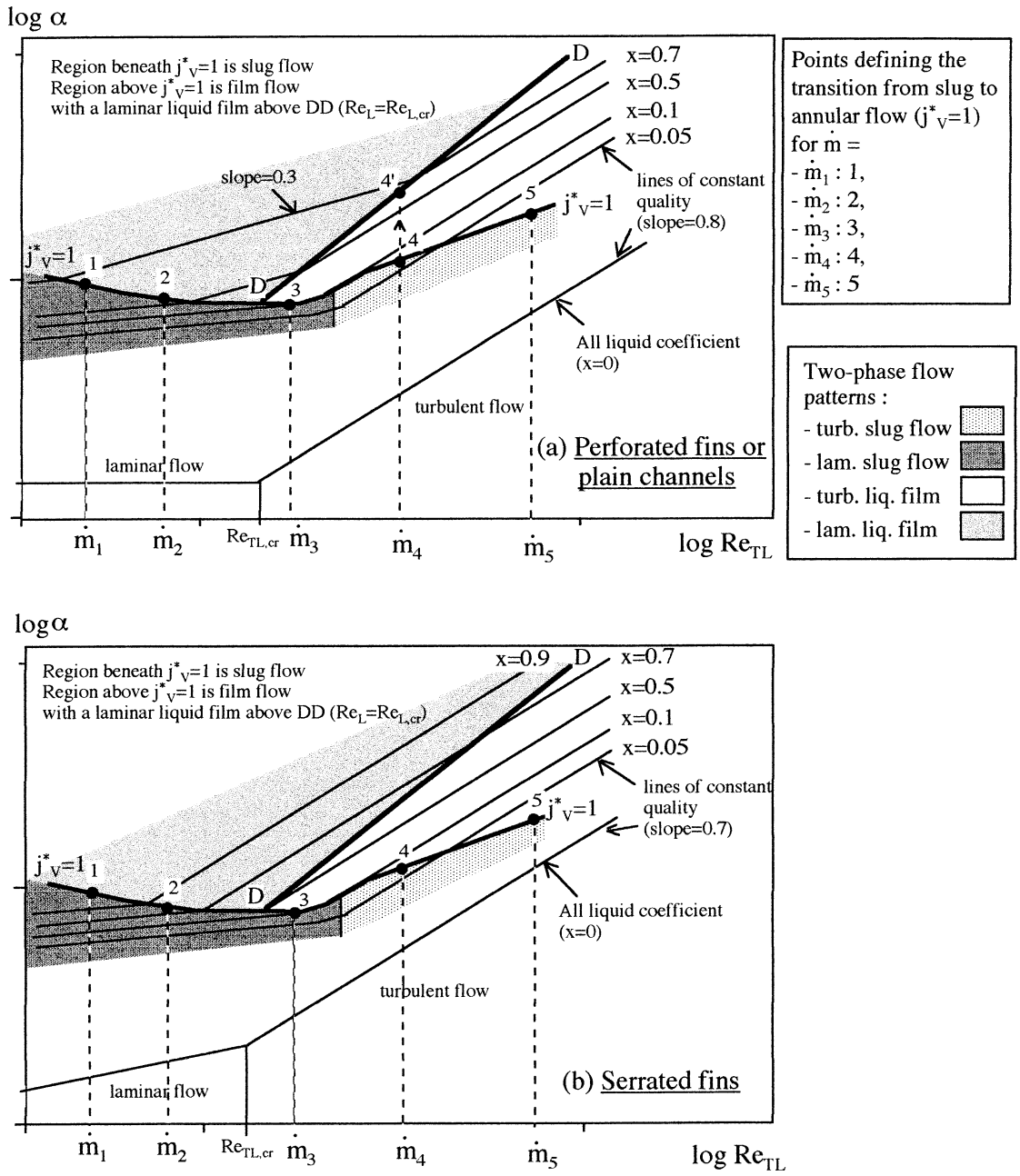

Fig. 7. Main heat transfer trends obtained in the slug and annular flow regions against Re_{TL}. Trends deduced basing in part on: (a) [31,32], (b) [12,13,33].

rated fin geometry, the influence of mass flux on F, for fixed X, seems to be more or less high according to the fluids used in the studies [4,31,32,34] (Table 1). Moreover, it is interesting to underline that in the slug flow region, for a given $1/X$, F is greater than the corresponding F-parameter in case of an annular flow.

According to Robertson [12] and Robertson and Wadekar [34] (Table 1), the enormous effect of vapour quality on the boiling heat transfer coefficient for vapour quality from zero to approximately 5% is due to the fact that, at the onset of boiling, nucleation may create bubbles of a size almost large enough to span the channel and these bubbles then grow by evaporation of the film surrounding them. This rapid production of vapour bubbles just after the onset of boiling will essentially increase the velocity of the two-phase. Moreover, because of their proximity to one another in the small passages, these bubbles will introduce an "entrance effect" and thereby recreate temperature and velocity profiles thus producing a sudden and considerable increase in heat transfer coefficient as convective boiling establishes between all liquid and 5% vapour quality. As the void fraction increases with increasing quality, the bubbles will coalesce, spanning the narrow passages to form slug flow for vapour quality higher than approximately 5%. Under these circumstances, the larger bubbles will produce longer lengths of uninterrupted liquid, hence the

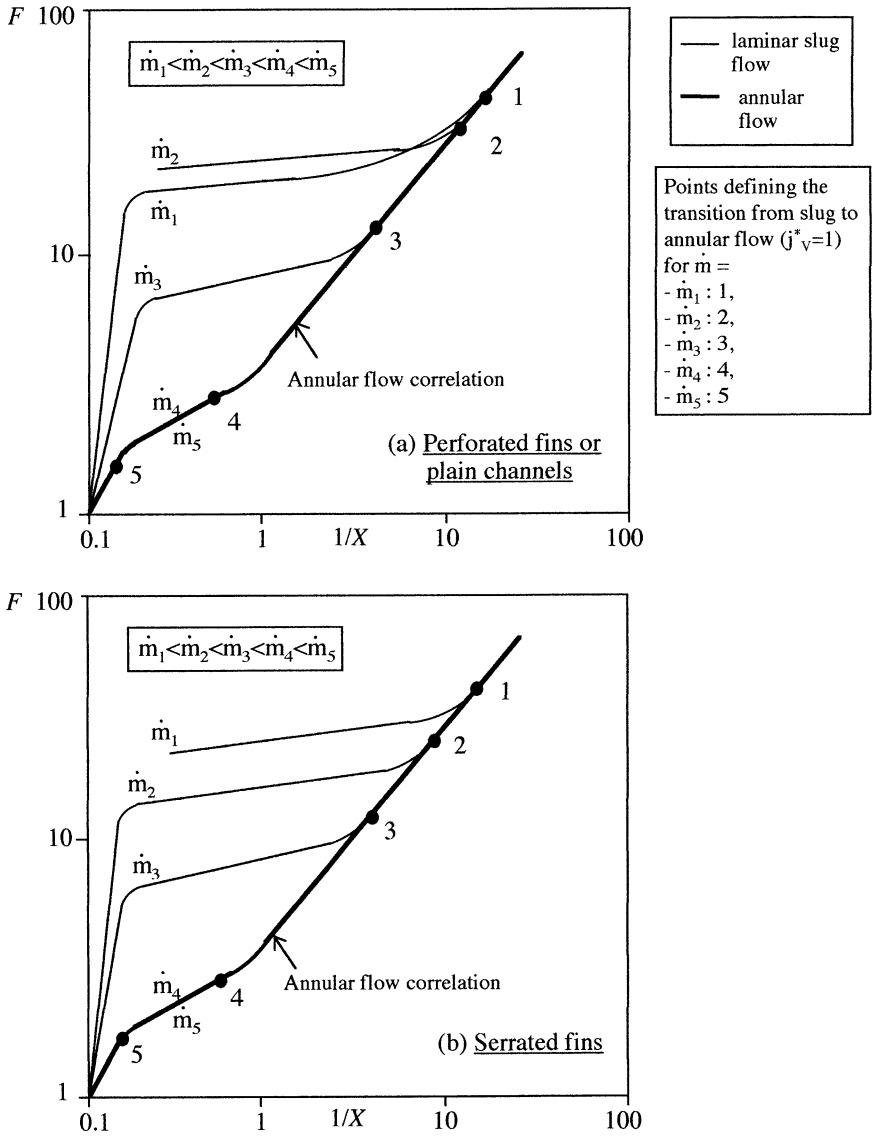

Fig. 8. F against $1/X$ in the slug and annular flow regions. Trends deduced basing in part on: (a) [4,10,31,34,42,69–71], (b) [2,36].

'entrance' effect will disappear, the liquid film thickness will be constant and the heat transfer coefficient will be only weakly dependent on vapour quality once the slug flow is established. Moreover, according to Carey [73], the high heat transfer coefficients obtained in the slug flow region in compact offset fin geometries may be due to the effects of surface tension on vapour motion through the fin matrix (see Section 5.6).

5.1.2. Analysis in annular flow region

Always in forced-convective boiling, the trends of the boiling heat transfer coefficients obtained in the annular flow region, corresponding to $j_V^* > 1$, in the laminar and turbulent film flow regions, for small passages, are shown in Figs. 6, 7 and 8. They are deduced from the experimental heat transfer characteristics obtained by different authors on the one hand, and by basing on Chen's [65] formulation, during film flow evaporation, to express the convective boiling heat transfer coefficient on the other hand, as it will be explained afterwards.

In the annular flow region, obtained for higher vapour qualities than the slug flow, the heat transfer coefficient appears to increase more rapidly with increasing vapour quality (Fig. 6) and mass flux (Fig. 7) (Robertson and coworkers [12,13,31–34], other authors [1,2,37] (Table 1)). Moreover, for high enough mass fluxes (for example $\dot{m}_4$, $\dot{m}_5$), coefficients all tend to be proportional to Re_{TL} to the power of 0.8 approximately, corresponding to an annular flow with a turbulent liquid film [12,31–33] (Table 1). Robertson [12] correlated his data obtained on a serrated-fin test section for an annular flow with a turbulent liquid film by: $\alpha = 375\dot{m}^{0.8}x$ W·m^{-2}·K^{-1} for $x > 0.3$ and by: $\alpha = \dot{m}^{0.8}(160x + 66)$ W·m^{-2}·K^{-1} for $x < 0.3$, showing as in Fig. 6(b) for mass fluxes $\dot{m}_4$ and $\dot{m}_5$ that there is a steep increase in the heat transfer coefficient with vapour quality in the annular region above a critical value of vapour

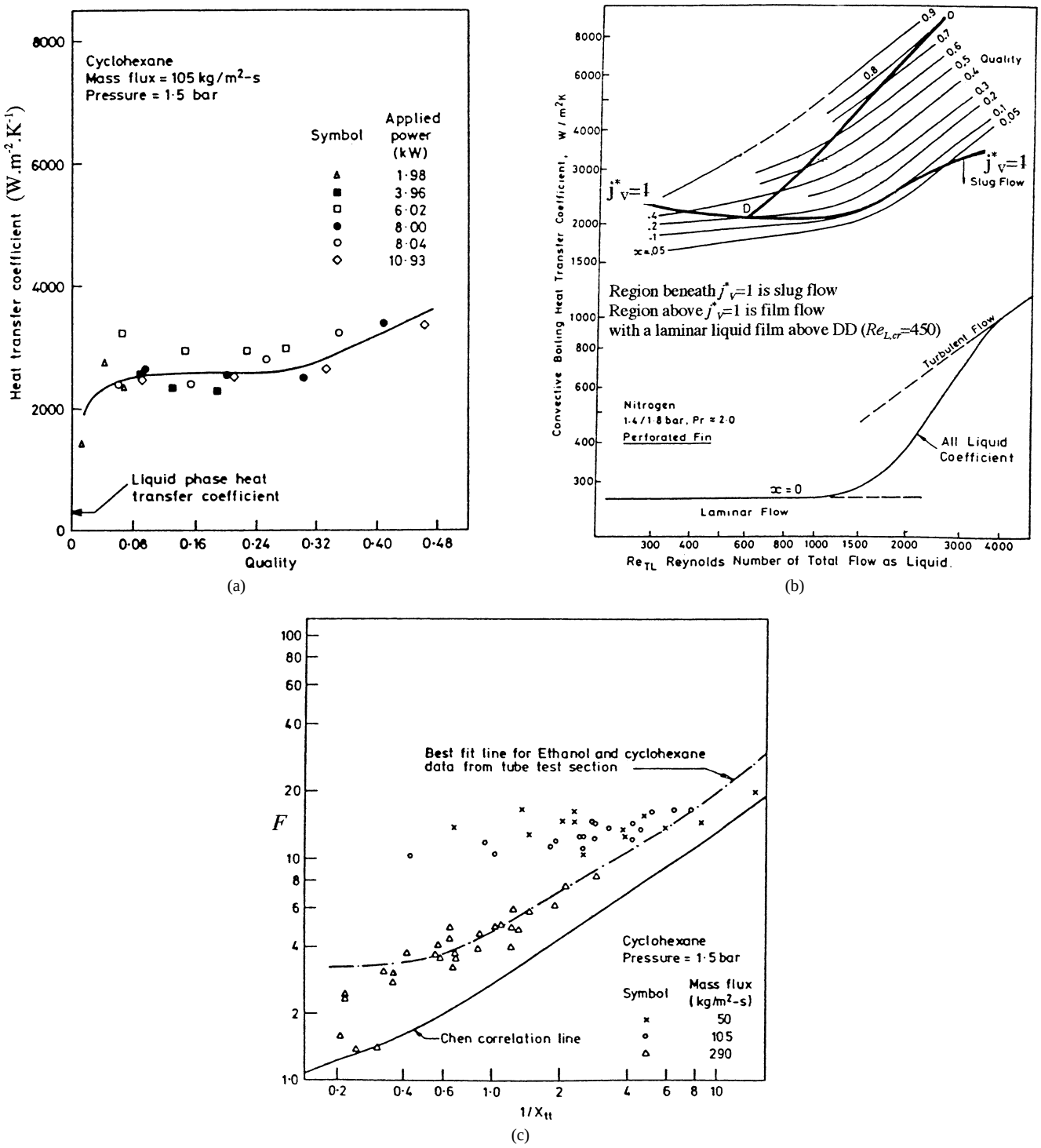

Fig. 9. Experimental heat transfer characteristics obtained on perforated fin test sections: (a) α against x, Robertson and Wadekar [34] data (Table 1), (b) α against Re_{TL}, Robertson and Clarke [32] data (Table 1), (c) F against $1/X_{\mathrm{tt}}$, Robertson and Wadekar [34] data (Table 1).

quality. The linear variation of α with vapour quality in this region reflects the progressive thinning of the liquid film. In the annular flow region, Robertson and Clarke [32] deduced that below liquid critical Reynolds number $Re_{L\mathrm{cr}}$ depending on the fin geometry and test fluid ($Re_{L\mathrm{cr}} = 450$ for $Pr_L = 2$ in Robertson and Clarke's study [32], Fig. 9(b)), that is the region above line DD in Fig. 7, laminar film flow exists. Below DD ($Re_L > Re_{L\mathrm{cr}}$), the film is not laminar. For example in Fig. 7(a), for fixed mass flux $\dot{m}_4$, when vapour quality increases, Reynolds number Re_L decreases, the characteristic point moves in the turbulent liquid film flow region from point 4 to point 4' at which Re_L is equal

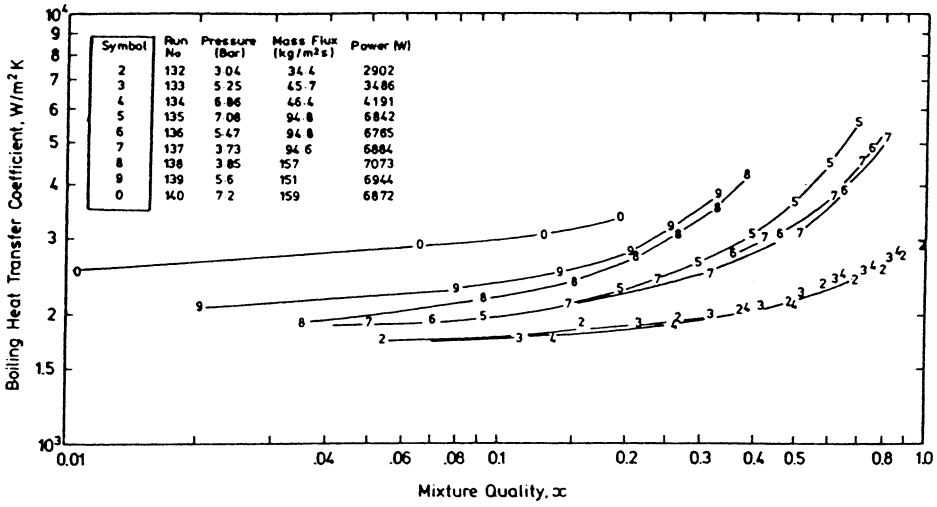

(a)

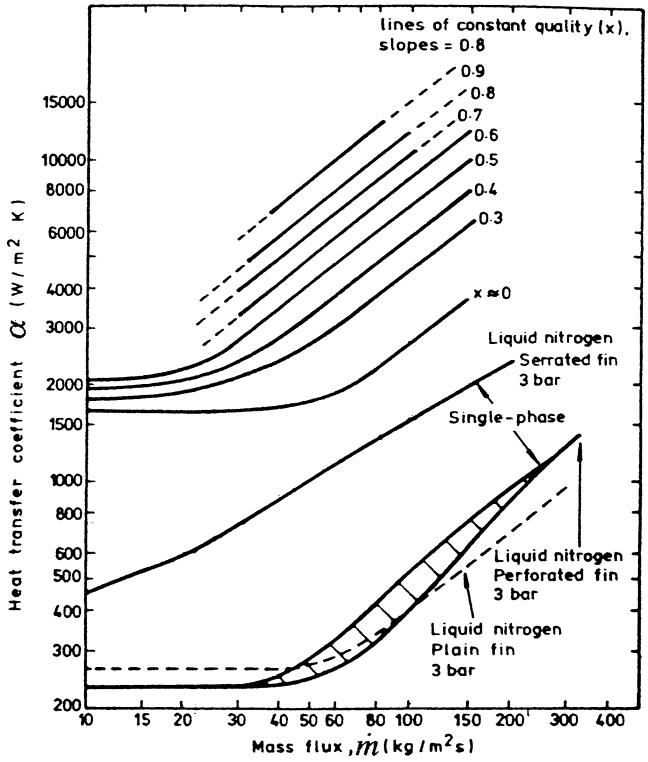

(b)

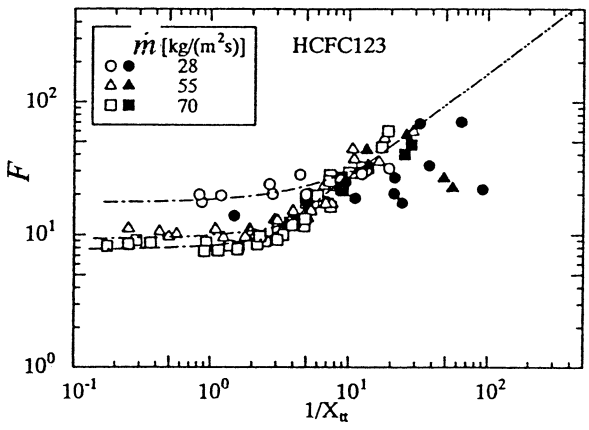

(c)

Fig. 10. Experimental heat transfer characteristics obtained on serrated fin test sections: (a) α against x, Robertson and Lovegrove [13,33] data (Table 1), (b) α against $\dot{m}$, Robertson [12] data (Table 1), (c) F against $1/X_{\mathrm{tt}}$, Koyama et al. [36] data (Table 1).

to $Re_{L\mathrm{cr}}$, and when Re_L becomes lower than $Re_{L\mathrm{cr}}$, the liquid film flow becomes laminar. In the representation of the heat transfer trends in terms of F over $1/X$ in Fig. 8, for a given mass flux (for example, $\dot{m} = \dot{m}_3$), F appears to increase more rapidly with increasing vapour quality in the annular flow region (on the right of point 3) than in the slug flow region (on the left of point 3). In the annular flow region, F tends to be independent of mass flux and plotting F against $1/X$ is a reasonable method for correlating all the convective boiling data in the annular laminar and turbulent flow regions. Furthermore, Wadekar [4], Robertson and Wadekar [34] observed that their data on their perforated fin test section (Table 1) in the turbulent annular flow region were very similar to those obtained from a round tube.

Besides, we completed the previously described boiling heat transfer trends in the annular flow region by adopting

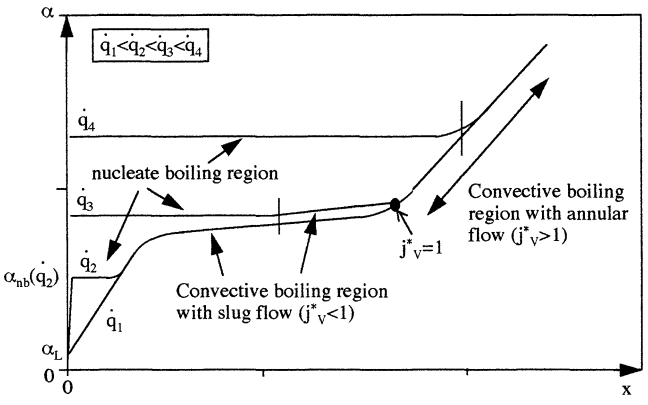

Fig. 11. Main boiling heat transfer trends obtained in the nucleate and convective boiling (annular and slug flow) regions, for a given mass flux. Trends deduced in part basing on [23,42].

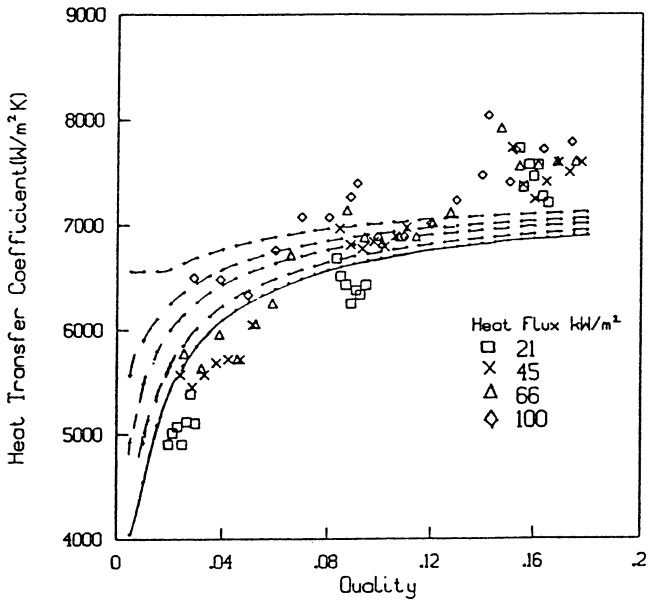

Fig. 12. Comparison of predictions of Wadekar's model [23] with measured data of Kenning and Cooper [42] at 65 kg·m^{-2}·s^{-1} mass flux and 170 kPa pressure (Table 2).

Chen's [65] formulation, Eq. (5) to express the convective boiling heat transfer coefficient. By both empirical correlation of heat transfer data and a heat-momentum transfer analogy analysis, Chen [65] showed that the F-factor could be exclusively correlated by the Lockart–Martinelli parameter X. In particular, Chen's [65] convective heat transfer data are correlated by the following equation [42]:

$$F = 1 + 1.8(1/X)^{0.79} \tag{9}$$

Thus, for perforated fin test sections or plain channels, the slope of 0.3 in the laminar film flow region and 0.8 in the turbulent film flow region observed for the log–log plot of heat transfer coefficient against Re_{TL} in Fig. 7(a) and the trends of heat transfer coefficient against vapour quality in the annular flow region in Fig. 6(a) are deduced using Eq. (5) for α and (9) for F. To determine α_L and f according to Eqs. (6) and (8) respectively, correlations such as those given by Shah and London [74] in the laminar flow region and Dittus-Boelter and Blasius in the turbulent flow region are used. For serrated fin test sections, the slope of approximately 0.7 in both the laminar and turbulent film flow regions observed in Fig. 7(b) and the trends of heat transfer coefficient against vapour quality in the annular flow region in Fig. 6(b) are deduced using correlations such as those given by Wieting [75] to determine α_L and f in the laminar and turbulent flow regions.

5.2. Effect of nucleate boiling on heat transfer trends

Taking the effect of nucleate boiling on heat transfer coefficient into account, the typical trends of boiling heat transfer coefficient against vapour quality, for different heat fluxes and a given mass flux, are given in Fig. 11. These trends have been deduced in part basing on measured data of Kenning and Cooper [42] for flow boiling of water in a 14.4 mm diameter tube test-section (Table 2) and the results given by Wadekar's [23] model, both shown in Fig. 12. For the lower heat fluxes ($\dot{q}_1$), convective boiling is predominant over the entire vapour quality range and the same trend as shown in Fig. 6 is obtained. For higher heat fluxes ($\dot{q}_2, \dot{q}_3, \dot{q}_4$), nucleate boiling is predominant for lower vapour qualities and convective boiling with a slug or annular flow becomes predominant for larger vapour qualities.

5.3. Effect of channel dimensions in the annular flow region

It must be underlined that the influence of channel dimensions in the annular flow region is not exactly the same on the boiling heat transfer coefficient as on the F factor, since $\alpha = F\alpha_L$, with α_L estimated by Eq. (6) and thus proportional to D_h^{-n} $(0 < n \leqslant 1)$. It is deduced from different studies that, for small enough passage sizes, with a decrease in channel dimensions, the heat transfer coefficient in the annular flow region increases, due to the reduction of the liquid film flowing on the heated surface [76,77], whereas for larger channels, the heat transfer coefficient becomes less sensitive to changes in channel dimensions.

In particular, Mandrusiak and Carey [2] tested three different large scale offset-strip fin geometries with the same interruption length and different fin heights (Table 1). Relative to the effect of the passage size on the boiling heat transfer coefficient, for the passage hydraulic diameters ranging from 3 to 9 mm, the heat transfer coefficient during annular film-flow evaporation was observed to be only weakly dependent on the passage size. For a given quality and mass flux, the heat transfer coefficients for the three surfaces differed only by about 20%. According to the authors, the three large scale offset fin geometries were sufficiently similar that the overall two-phase heat transfer coefficient was not very sensitive to changes in fin dimensions. In their study, also the F-factor data appeared relatively insensitive to differences in channel dimensions

for the three surfaces. Feldman [37,38] examined the effect of the fin spacing of perforated fins on the boiling heat transfer coefficient by comparing the results obtained with 0.95 mm spaced fins (perf3) (Table 1) and 1.21 mm spaced fins (perf1). For a given quality and mass flux, in the convective boiling region, the heat transfer coefficients for the two fin spacings did not differ. Oh et al. [10] examined the effect of capillary tube diameters on the boiling heat transfer coefficient by comparing the results obtained with 1.0 and 2.0 mm diameter tubes (Table 2). They observed that the heat transfer coefficient of the 1.0 mm tube was higher than that of the 2.0 mm tube up to the vapour quality 0.6. They also noticed that in the forced convection region, the F parameter plotted against $1/X_{tt}$ (indeed, for their test conditions, $X = X_{tt}$) was independent of tube diameter. Cornwell and Kew [3] (Table 2), Bar Cohen and Schweitzer [78] found that for the annular flow regime, there was virtually no effect of the spacing on the F factor or the heat transfer coefficient, as long as the Confinement number Co remained lower than 0.5. Indeed, Bankoff and Rehm [61] in their study of flow in annuli at high Co values found that the F factor needed to be modified to considerably higher values to describe the convective evaporation.

5.4. Effect of fin geometry in compact plate-fin heat exchangers

For single-phase heat transfer applications, among the different geometries of plate-fin heat exchangers, the offset-strip fins provide one of the highest performances because they maintain thin boundary layers on the fins. According to Robertson [12] (Table 1), the high heat transfer coefficients associated with the single phase region in serrated fin passages are caused by the interruptions to the development of transverse temperature and velocity profiles (the entrance-length effect) produced by this form of finning.

In forced-convective boiling, the serrated-fins are also expected to give higher heat transfer coefficients than plain fins. According to Carey [5], the use of small scale enhanced passages, like serrated or perforated plate-fin passages (Fig. 2) can substantially enhance the performance of a compact evaporator or condenser. By comparing the heat transfer coefficients obtained by Feldman [37,38] for offset-strip fins (osf1) and perforated fins (perf1) in the convective boiling region for similar experimental conditions and fin dimensions (Table 1), it is deduced that heat transfer coefficients for offset-strip fins are higher than those for perforated fins. Feldman [37,38] also examined the effect of fin length of offset-strip fins L_f on the boiling heat transfer coefficient by comparing the results obtained with fins 3.18 mm long (osf1) and 9.52 mm long (osf2). The heat transfer coefficients obtained for the 3.18 mm long fins are about 35% higher than those obtained for the 9.52 mm long fins. Mandrusiak and Carey [2] obtained that the measured boiling heat transfer coefficients in their offset-fin channels (Table 1) were typically two to three times the values predicted by the Bennett and Chen [79] correlation for a round tube with the same hydraulic diameter. Hence their geometries provide substantial enhancement of the flow boiling heat transfer performance relative to that for a round tube under comparable conditions. In a comparison of offset-strip fin [12] (Table 1) and perforated fin passages [31] (Table 1), values of the heat transfer coefficient are similar at low qualities, while at high qualities the heat transfer coefficient can be 50% higher for the offset-strip fin geometry. According to Robertson and Clarke [32] (Table 1), the reason for the similarity of heat transfer coefficients with serrated and perforated fins at low quality is the presence of the same two-phase flow pattern, slug flow. According to Robertson [12], Robertson and Clarke [32], the higher heat transfer coefficients apparent during annular flow boiling on the serrated fins would be the result primarily of the relative thinness of the liquid film flowing along each fin from leading to trailing edge where it is disrupted, at high vapour qualities, into the form of a spray and then reformed on the following fin. Thus, a thinner liquid film can be expected on the serrated-fin in comparison with other forms of finning.

5.5. Effect of gravity (orientation)

As underlined in Section 3.6, gravity effects, resulting from channel orientation, are important in phase-change heat transfer in large channels because they can influence flow patterns, and thereby heat transfer. Especially, some authors [11,14] (Table 2), [62–64] noticed that, because of the loss of wetting in horizontal flow at low mass fluxes (for example, in wavy-stratified flows), there was a loss of convective heat transfer area, thereby decreasing the heat transfer coefficient compared with the results in the annular flow regime for similar test conditions. It was shown by several authors [14] (Table 2), [62–64,80,81] that the correlation of data in horizontal flow requires the inclusion of the Froude number to account for gravitational effects. In their experimental studies of flow boiling in horizontal tubes (Table 2), Wattelet et al. [11,14] underlined that there was no major effect of vapour quality on heat transfer coefficient in the wavy-stratified flow regime, whereas in the annular flow regime, the heat transfer coefficient increased with vapour quality.

In small channels, as surface tension forces dominate gravity forces (see Section 3.6), the gravity does not exert influence on the flow pattern inside tubes any more. Carey and co-workers [2,35] compared horizontal and vertical flow boiling data for the same offset-strip fin geometry (Table 1) and showed that the boiling heat transfer coefficients were in good agreement.

5.6. Effect of surface tension for an offset-strip fin geometry

Carey [73] studied the role of surface tension on heat transfer in a low vapour quality and low flow rate channel characterised by offset-strip fin surface. He presented a

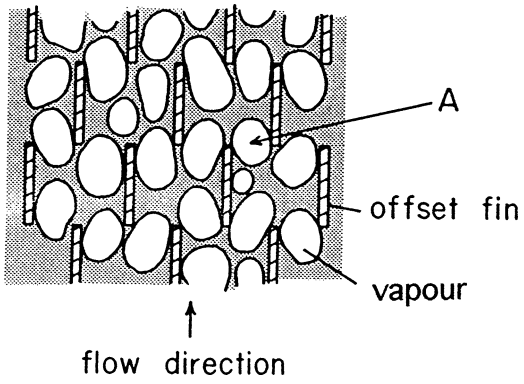

Fig. 13. Schematic cross section of two-phase flow through an offset strip fin array at low quality (Carey [73]).

schematic cross section of a slug flow of water and air through an offset fin matrix (Fig. 13). It can be seen that vapour bubbles must squeeze through the narrow passage where one fin ends and another begins. When the liquid–vapour interface contacts the fin, surface tension forces will affect the bubble motion. A bubble at the narrow passage *A* can only pass through if there is a net downstream force on the bubble. Carey [73] made the balance of forces acting on a vapour bubble flowing in the fin matrix and deduced that a minimum value of void fraction and hence a minimum value of the heat transfer coefficient (according to the Chilton–Colburn analogy) was required before the downstream force due to the friction pressure gradient acting across the bubble could overcome the surface tension and buoyancy forces acting on the bubble and push the bubbles through the matrix. If the void fraction is below this minimum value, bubbles will be held back until vapour generation raises the void fraction to the required minimum value. This explains why, at low flow rates, in the slug flow region, the surface tension has a retarding effect on vapour motion and the boiling heat transfer coefficients appear to level off at a minimum value as x tends towards zero (Fig. 6). This enhancement of heat transfer was found to be consistent with trends in convective boiling heat transfer data obtained by Robertson [12] and Robertson and Lovegrove [13] (Table 1).

According to Carey [5], for annular flow in small-scale finned surfaces, surface tension also produces the Gregorig effect in which liquid is drawn into corner regions because of pressure gradients induced by changes in curvature of the interface. The Gregorig effect acts to make the liquid film thicker in the corner regions and thinner in the centre of flat surfaces in the passage. This serves to enhance convective boiling heat transfer in finned surfaces if sufficient liquid is present to keep the surfaces fully wetted. If, on the other hand, the thinned portions of the film become locations where premature dryout occurs, the Gregorig effect may decrease heat transfer performance of the surface.

6. Characteristics of nucleate flow boiling in small channels

Nucleate boiling is observed to be the predominant heat transfer mechanism (characterised by a heat transfer coefficient dependent on heat flux and independent of mass flux and vapour quality), for three flow patterns:

- the isolated bubbles flow,
- the confined (or coalesced) bubbles flow, in which case the heat transfer mechanism is more specifically called “the confined bubble boiling” rather than nucleate boiling by Kew and Cornwell [9] (Table 2),
- the slug flow in some studies.

As examples of flows observed in the nucleate boiling region, according to Wambsganss et al. [24] (Table 2), the thick-liquid regions of slug flow were more likely to support nucleation than the thin liquid films of annular flow. In the study of Feldman [37] (Table 1), the flow observed was the isolated or confined bubbles flow. Indeed, for her tests, the Confinement number remained equal to 0.5 which corresponds to the transition criterion used by Cornwell and Kew [3] (Table 2) to distinguish the confined bubble regime from the isolated bubble regime. In other studies [16,45, 47,48] (Table 3), according to the channel dimensions, as explained in the next section with more details, the flow was either the isolated bubbles flow or the confined bubbles flow.

In the coalesced bubble and slug flow regions, the heat transfer mechanism is categorised as nucleate boiling due to the dependence of heat transfer coefficients on heat flux. More precisely, researchers [9,20] (Table 2), [16,45, 48] (Table 3), [58,61,76,77] concluded that thermal transport was due mainly to two mechanisms: conduction through and evaporation of the thin liquid film which appeared when a bubble passed by the heated surface, and the sensible heat transport caused by substitution of the superheated liquid swept away by the bubble with the liquid at bulk temperature after the bubble transit. In particular, Ishibashi and Nishikawa [45] (Table 3) considered that heat transfer mechanism in the coalesced bubble region was due to periodical displacement of the liquid with the bubbles, based on the observation of bubble generating behaviour. They showed that in the coalesced bubble region, bubble emission frequency N controlled the boiling heat transfer mechanism. For given fluid and space dimension, they established that the heat transfer coefficient was proportional to $N^{2/3}$. According to Kew and Cornwell [9] (Table 2), the proportion of the tube length which is occupied by bubbles at any one time is a function of the heat flux, which determines the propensity of bubbles to nucleate on the wall and the net rate of vapour generation. The processes are thus similar to those occurring during nucleate pool boiling, except that the bubbles are constrained during their expansion. The work of Aligoodarz and Kenning [82] involved measurement of the variation in wall superheat during the passage of a sliding

coalesced bubble through a narrow channel. They observed that the temperature variations were similar to those due to microlayer evaporation under pool boiling bubbles.

6.1. Effect of channel dimensions on heat transfer characteristics and associated flow patterns

Studies in small channels or confined spaces have demonstrated that channel dimensions can have a critical role in determining heat transfer mechanisms and a strong effect on the heat transfer coefficient. At a given heat flux, it is deduced from many investigations [3,8,17,20,25] (Table 2), [16,45–50] (Table 3), [27,29,58,59,77,83] that there is a critical size below which boiling heat transfer is enhanced as the channel or gap size further decreases. Above that critical size, there is nearly no influence of channel size on heat transfer. For example, for flow boiling in annuli, Aritomi et al. [50] (Table 3) observed that boiling heat transfer increased with a decrease in the channel gap for gaps smaller than 2 mm, whereas for bigger gaps, it was not influenced by the gap size any more. Xia et al. [16] and Mertz et al. [49] (Table 3) determined a critical size approximately equal to 3 mm. Most of the authors observed that nucleate boiling was greatly intensified in a small channel and that the wall superheat for flow boiling might be much smaller than that of larger tubes for the same wall heat flux. For example, about nucleate boiling in annuli, Aoki et al. [47] (Table 3) found that as the gap width decreased, the boiling curve shifted to the left and the heat transfer coefficient increased.

In fact, at a given heat flux, as the channel dimension is reduced, the flow pattern progressively passes from an isolated bubbles flow to a confined bubbles regime (see Section 3.4.1) and among the previous authors, most of them have concluded that while little enhancement of heat transfer coefficient can occur in the isolated bubble region, it is most pronounced in the confined bubble region. Therefore, the critical size defining the changes in heat transfer trends coincides with the one defining the transition between the isolated bubble and confined bubble regimes. For example, according to Ishibashi and Nishikawa [45] (Table 3), Nishikawa and Fujita's [59] results about nucleate boiling in annuli, in the isolated bubble regime for a clearance more than 3 mm, the heat transfer coefficient is proportional to $s^{-0.13}$, whereas in the confined bubble region for a space dimension less than 3 mm, it is proportional to $s^{-2/3}$. Fujita et al. [48] obtained in their experimental study of nucleate boiling heat transfer in narrow space between rectangular surfaces (Table 3), at gaps of 2 and 0.6 mm, that an isolated bubble at low heat flux was squeezed and flattened and grew rapidly to cover the width of the heating surface, enhancing heat transfer markedly in comparison with an unconfined space. For flow boiling in a rectangular channel, in the isolated bubble region, Cornwell and Kew [3] (Table 2) suggest that $\alpha = f(s^{-0.2})$. Moreover, the same authors [3,58] have introduced the Confinement number *Co* for taking into account of heat transfer increase produced by a small channel dimension. They suggest that the effects of confinement are significant for channels having hydraulic diameters such that the confinement number is in excess of 0.5. Thus, that criterion allows to determine the value of the critical size of the channel defining the transition between the isolated bubble and confined bubble regimes and below which heat transfer is influenced by gap size, for given fluid and pressure.

Enhancement of heat transfer in small channels as compared with larger ones was attributed to the increased bubble activity or the microlayer of liquid beneath the bubble becoming thinner with a decrease in the gap size hence contributing to an increase in sensible heat transport, to the removal of the superheated liquid carried out by the bubble transit along the heated surface and an associated increase in evaporation rate of this film [16,45–48,50] (Table 3) [77,84]. More precisely, according to Ishibashi and Nishikawa [45] (Table 3), the heat transfer coefficient in the coalesced bubble region is increased by the forced tearing off of the boundary layer due to the bubbles. Aritomi et al. [50] (Table 3) underlined that the number of bubbles departing from the heated wall increased inversely with the cross-section of the channel. Consequently, the turbulence induced by bubble departure was enhanced. Fujita et al. [48] (Table 3) explained that at lower heat flux, the heat transfer was enhanced due to the two-phase mixture agitation in a narrow space. Jensen et al. [46] (Table 3) showed that the much larger vapour masses observed in the confined portions than in the unconfined portion were responsible for higher heat transfer coefficients. Moreover, according to Chernobyl'skii and Tananaiko [84], probably in the isolated bubble region, the increase of heat transfer coefficient with reduced space dimension is due to the fact that the size of the vapour bubbles is reduced, the turbulence of the flow is increased and the overall vapour content of the mixture rises. The trajectories of the small vapour bubbles are transferred to the periphery and the liquid is violently agitated: this leads to a high rate of heat removal from the heated wall.

Nevertheless, several authors concluded that, at fixed moderate heat flux, the heat transfer coefficient increased up to a certain maximum value with decrease of the gap size, while degradation occurred for a further decrease of the gap size [3,20] (Table 2), [16,46,48] (Table 3), [85]. For example, the variation of the boiling heat transfer coefficient with gap size and the boiling curves obtained experimentally by Xia et al. [16] are presented in Fig. 14(a) and (b), respectively. Basing on the previous authors' results on boiling heat transfer in narrow channels, the heat transfer coefficients trends against gap size s for different heat fluxes are presented in Fig. 15(a). s_3 represents the critical size defining the transition between the isolated bubble and confined bubble regimes. For low heat flux (for example, $\dot{q}_1$), the heat transfer coefficient is enhanced with a decrease in the gap size. For higher heat flux $\dot{q}_2$, with decreasing gap size, the heat transfer coefficient increases first, then decreases. For still higher heat flux ($\dot{q}_3$), heat transfer is

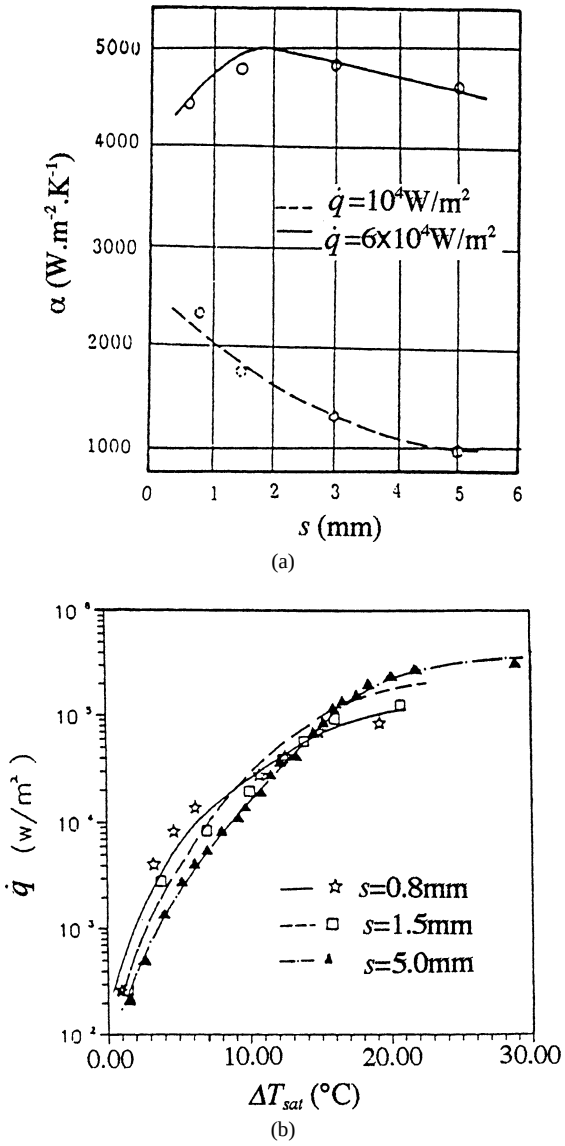

Fig. 14. Experimental data of Xia et al. [16] (Table 3): (a) Variation of boiling heat transfer coefficient with gap size, (b) Influence of gap size on boiling curve.

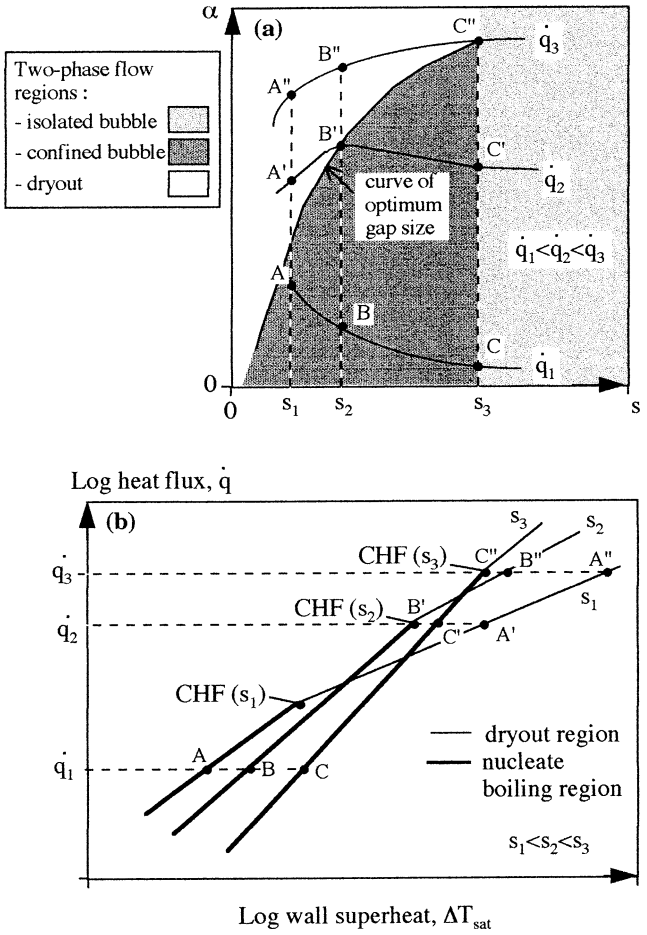

Fig. 15. Effect of gap size on (a) heat transfer coefficient, (b) boiling curve. Trends deduced in part basing on [3,8,16,17,20,25,27,29,45–50,58,59,77, 85].

degraded with a decrease in the gap size. Therefore, there exists an optimum gap size depending on heat flux (equal to s_2 for heat flux $\dot{q}_2$, for example) at which the boiling heat transfer coefficient reaches its maximum. As shown in Fig. 15(a), this optimum gap size increases with heat flux. According to the previous researchers, for fixed heat flux, the decrease in heat transfer coefficient with the reduction of gap size below an optimum value is due to the transition at this optimum value from nucleate boiling to dryout region, reducing the heat transfer as compared with larger gap sizes. For example, in their experimental study of nucleate boiling in a vertical narrow space, Fujita et al. [48] (Table 3) obtained that for gap size $s = 0.15$ mm, the heat transfer rate was less than for larger gap sizes or unconfined boiling, because most of the heating surface was covered with vapour and the wetted area was very small compared with the total heating surface.

6.2. *Effect of heat flux—Correlation for heat transfer coefficient*

The major part of the researchers [7,25] (Table 2), [45, 49] (Table 3), [59,68,86] who worked in the nucleate pool or flow boiling region, whatever the geometry of the exchange surface, found that their data could be reasonably correlated with a power function relationship between heat transfer coefficient and heat flux (Fig. 4(c)):

$$\alpha_{\mathrm{nb}} = C\dot{q}^{n} \tag{10}$$

with

$$\dot{q} = \alpha_{\mathrm{nb}}\Delta T_{\mathrm{sat}} \tag{11}$$

where C and n are functions of geometry, size, fluid properties and pressure.

These data can be correlated with a power function relationship between heat flux and wall superheat as well, by combining Eqs. (10) and (11) (Fig. 5):

$$\dot{q} = C^{1/(1-n)}\Delta T_{\mathrm{sat}}^{1/(1-n)} \tag{12}$$

It has been shown [68] that the heat transfer coefficient in purely nucleate flow boiling in large channels is similar to that in pool boiling for the same fluid at the same pressure. According to the authors who studied nucleate boiling in large tubes [68,86,87] and several others in narrow spaces [7, 25] (Table 2), [45,49] (Table 3), exponent n remains between 0.50 and 0.75. Kew and Cornwell [9] (Table 2) deduced, concerning their measured boiling heat transfer coefficients in single, small-diameter tubes (Table 2), in the confined bubbles flow region, that simple nucleate pool boiling correlations, such as that of Cooper [68], best predicted the data. They observed that boiling heat transfer processes in narrow tubes were similar to those occurring during nucleate pool boiling, except that the bubbles were constrained during their expansion. It is therefore logical that correlations like nucleate pool boiling correlations (with C depending on channel dimensions) give reasonable results when applied to narrow tubes. Ishibashi and Nishikawa [45] (Table 3) also obtained with several fluids (water, sodium oleate and saponin) that in the coalesced bubble region as in the isolated bubble region in their annuli, the relation between heat transfer coefficient and heat flux was expressed by Eq. (10), with $n = 2/3$.

Nevertheless, for large enough heat fluxes, several authors [3] (Table 2), [16,48,49] (Table 3), [27,85] found that the slope of the boiling curve (log–log plot of heat flux against wall superheat) for nucleate flow boiling in small channels, equal to $1/(1-n)$, became weaker than for large tubes. In particular, Galezha et al. [27] who suggested a nucleation-dominant mechanism for their test conditions with offset strip fin surfaces showed that the heat transfer coefficient varied with heat flux to approximately the one-third power. Cornwell and Kew [3] (Table 2) also found that for their tests with R113 (Table 2) the heat transfer coefficient varied with heat flux to approximately the one-third power. In Fujita and Uchida [85] for water boiling between plates at various spacings, it can be seen that exponent n varies from 0.7 for the unconfined state to 0.3 for $Co = 0.6$. In fact, by referring to the previous section and the interesting study of Xia et al. [16] (Table 3, Fig. 14), these results can be interpreted. Basing on the previous authors' results on boiling heat transfer in narrow channels, beside the heat transfer coefficients trends against gap size s presented in the previous section (Fig. 15(a)), the typical trends of the boiling curves for different gap sizes are presented in Fig. 15(b). By referring to the explanations given in the previous section, it is expected that the decrease in the slope of the boiling curve with the decrease in gap size at high enough heat fluxes, as shown in Fig. 15(b) is due to transition from nucleate boiling to dryout region when reducing the gap size at a fixed heat flux. These interpretations are confirmed by the results of Fujita et al. [48] (Table 3). Indeed, in narrow gaps of 2 and 0.6 mm, at high heat flux, they deduced that bubble generation became more frequent and stable than at low heat flux. Partial bubble accumulation was observed on the upper part of the heating surface, which reduced the slope of the boiling curve as compared with larger spaces and therefore the enhancement rate of heat transfer as compared with low heat fluxes. Ishibashi and Nishikawa [45] also obtained for their tests with ethyl alcohol (Table 3) that below a critical heat flux CHF (heat flux required to initiate dryout), in the coalesced bubble region, coefficient n was equal to $2/3$, whereas above that critical heat flux, coefficient n became equal to 0.12.

The trends of the boiling curves in Fig. 15(b) have been deduced also by inspecting the fact that critical heat flux CHF decreases with the reduction of gap size, which was observed by various authors [16,46–48] (Table 3), [78, 85]. For example, Jensen et al. [46] (Table 3) observed in confined annular geometries, decreases in CHF, compared to an unconfined tube, of up to a factor of 10. They developed a correlation relating the CHF at dryout to the geometry and to several fluid properties in which the CHF is proportional to clearance and inversely proportional to annulus length. At the opposite, surprisingly, according to Kureta et al. [44] (Table 2), Ammerman and You [83], in their experimental studies of forced flow boiling in small channels, the critical heat flux increases when channel size and heated length decrease.

6.3. Effect of channel geometry

Few studies dealing with the effect of channel geometry (circular or rectangular channels, plain or serrated-fin channels) on nucleate boiling heat transfer for channels of given hydraulic diameter have been found. Tran et al. [25] (Table 2) deduced from their experimental data that boiling heat transfer rates were comparable in small circular and rectangular channels of approximately the same hydraulic diameter, showing that there was no significant geometry effect for the two channels tested in the nucleate flow boiling region. Galezha et al. [27] reported the testing in the nucleate boiling region of four different offset-strip fin surfaces and one plain fin surface. The heat transfer coefficient was the highest for the surface having the shortest interruption length. A comparison of an offset-strip fin surface with a plain fin surface of the same geometry showed the boiling heat transfer coefficient to be higher with the offset-fin surface by approximately 50%.

6.4. Effect of surface tension

No experimental study evaluating the effect of surface tension on the nucleate boiling heat transfer except Ishibashi and Nishikawa's [45] (Table 3) was found. According to these authors, the effect of surface tension depends on the flow pattern. While surface tension was shown to have an effect on heat transfer coefficient in the isolated bubble region, in the coalesced bubble region, no surface tension effect was observed. They deduced that the bubbles were squeezed within a narrow space, and regardless of

surface tension, the behaviour of the generated bubbles was regulated by the heat flux and the space dimension.

6.5. Effect of pressure

As for surface tension, the effect of pressure on the nucleate boiling heat transfer coefficient was shown by Ishibashi and Nishikawa [45] (Table 3) to depend on the flow pattern. They observed the effect of pressure to be opposite in the isolated bubbles and confined bubbles regions. Indeed, they found that the increase in pressure, at a constant heat flux, caused the augmentation of heat transfer coefficient in the isolated-bubble region (α proportional to $p^{0.4}$) whereas it caused its diminution in the coalesced-bubble region (α proportional to $p^{-0.353}$).

7. Flow boiling heat transfer correlations

In compact heat exchangers, the heat transfer correlations are complicated by the strong dependence on channel size for some flow regimes. For large channels, many literature correlations, either correlations for one of the mechanisms, nucleate or convective boiling or correlations containing two terms, one for nucleation and one for convection, are available to predict the heat transfer coefficient. At the opposite, in compact heat exchangers, validated correlations are lacking. Some interesting correlations valuable in channels of small dimensions, in the convective or nucleate boiling regions, are reported in the following sections.

7.1. Convective boiling correlations (in the annular and slug flow regions)

Convective boiling correlations express the heat transfer coefficient as a function of fluid properties, mass flux, vapour quality and channel geometry/dimensions. The convective boiling correlations (in the annular or slug flow region) deduced from test data obtained by different authors are given in Table 4 with the geometries, tests conditions and fluids also reported. Almost all the authors obtain that their annular flow boiling data are reasonably correlated in terms of F and $1/X$ with, for most of them, $X = X_{tt}$ since their test conditions correspond to turbulent vapour and liquid phases.

In the convective boiling dominant region, for predicting his experimental boiling coefficients obtained from tests with nitrogen in perforated-fin channels, Robertson [31] (Table 1) proposed an empirical correlation of the form $F = 7X^{-0.36}$.

Carey [73] proposed a method of predicting forced convective heat transfer coefficients in offset fin heat exchanger geometries, in the slug and turbulent annular flow regions that accounts for surface tension effects in the slug flow region. This method was found to predict values of α which agreed well with the data of Robertson [12] and Robertson and Lovegrove [13] in the convective boiling region, for an offset-strip fin geometry (Table 1).

Mandrusiak and Carey [2] deduced that for all offset fin geometries considered in their study (Table 1), their data for turbulent annular film-flow evaporation were found to correlate well in terms of F factor and Martinelli parameter X_{tt}, using an approximate curve fit to their F-parameter data. Also in the same way, they correlated the measured values of Robertson [12] and Robertson and Lovegrove [13] (Table 1) in the turbulent annular film-flow region.

Troniewski and Witczak [41] correlated their experimental boiling data for the case of turbulent annular film flow evaporation of water in rectangular vertical and horizontal ducts (Table 2).

Chen [65] developed the first successful graphical relationship for convective flow boiling in vertical tubes of liquids with Pr_L close to unity. The Chen [65] prediction line of F-versus $1/X_{tt}$ was based on 594 data points, including water and five organics from six data sources, but the author did not propose any correlation for his prediction line. The latter was correlated later by Kenning and Cooper [42] (Table 2) in terms of F factor and Martinelli parameter X_{tt}. The Dittus–Boelter correlation was selected to evaluate α_L.

Kenning and Cooper [42] also correlated their own experimental data in the fully-developed convective heat transfer region, in the annular and slug/churn flow regions, for flow boiling of water in 9.6 and 14.4 mm diameter tubes (Table 2). The authors deduced that convection in the turbulent annular flow regime was well described by a modified Chen correlation. They also underlined that their correlation was inaccurate for liquids with large values of Prandtl number.

Wadekar [70] formulated a simple new correlation for the convective component of flow boiling heat transfer that predicts the data equally well for water, organic fluids and refrigerants, for both vertical and horizontal flows with channel geometries as different as tubes and plate-fin passages. This correlation relates the F factor to a parameter Y based on quality, reduced pressure and molecular weight in the turbulent annular flow region. With this approach, a knowledge of vapour phase density and viscosity is not required to calculate the two phase flow heat transfer coefficient. The inconvenience of this method is that it can be applied only to a flow with a turbulent liquid film.

Wattelet et al. [11] deduced that heat flux had minimal effects on their experimental data on boiling heat transfer coefficient in an horizontal circular tube in the turbulent annular flow regime (Table 2). They correlated their data using a purely convective relation where the F factor is only a function of X_{tt}.

7.2. Nucleate boiling correlations

Nucleate boiling correlations express the heat transfer coefficient as a function of heat flux, fluid properties, fluid pressure and channel dimensions. Kew and Cornwell [9] (Ta-

Table 4
Literature convective boiling correlations

Authors of correlations	Literature correlations	Data sources, Fluids	Geometries, test conditions
Robertson [31]	$F = 7X^{-0.36}$	Robertson [31], Nitrogen	Vertical perforated-fin geometry (Table 1), Annular flow, $60 \leqslant \dot{m} \leqslant 115$ kg·m^{-2}·s^{-1}, $0.03 \leqslant x \leqslant 0.8$ ($0.3 \leqslant 1/X \leqslant 30$), $1.45 \leqslant Pr_L \leqslant 2$
Carey [73]	In the slug flow region, $\alpha/\alpha_{L0} = Pr_L^{0.296}(1 + 0.34\Omega^{0.68})$ $\Omega = \left[\frac{2Re_{TL}^{0.198}}{\gamma_1 We}\left(\frac{D_h}{D_{hs}}\right)(1 - 0.25\,Bo)\right]^{1/2}$ $\gamma_1 = 1.136(L_f/D_h)^{-0.781}(\delta/D_h)^{0.534}$ D_{hs} = hydraulic diameter of small passage at end of fin $\alpha_{L0} = 0.242(L_f/D_h)^{-0.322}(\delta/D_h)^{0.089}(\lambda_L/D_h)\,Pr_L^{1/3}\,Re_{TL}^{0.632}$ *We* (Weber number) $= \dot{m}^2 D_{hs}/(\sigma\rho_L)$ *Bo* (Bond number) $= (\rho_L - \rho_V)g\,D_{hs}^2 \sin\theta/\sigma$ In the turbulent annular flow region, $F = Pr_L^{0.296} \times 1.65(1/X_{tt} + 0.60)^{0.78}$ $1/X_{tt} = (\nu_V/\nu_L)^{0.099}(\rho_L/\rho_V)^{0.401}(x/(1-x))^{0.901}$ for $1/X_{tt} > 0.1$ $\alpha_L = 0.242(L_f/D_h)^{-0.322}(\delta/D_h)^{0.089}(\lambda_L/D_h)\,Pr_L^{1/3}\,Re_L^{0.632}$ For any set of conditions, $\alpha = \max(\alpha_{slug}, \alpha_{annular})$	Robertson [12], Nitrogen Robertson and Lovegrove [13], R11	Vertical offset strip-fin geometry (Table 1), $Pr_L = 2 - 2.25$
Mandrusiak and Carey [2]	$F = \alpha/\alpha_{Lp} = Pr_L^{0.296}(1 + 28/X_{tt}^2)^{0.372}$ $1/X_{tt} = (\mu_V/\mu_L)^{n/2}(\rho_L/\rho_V)^{1/2}(x/(1-x))^{1-n/2}$ $\alpha_{Lp} = A(\lambda_L/D_{hp})\,Pr_L^{1/3}\,Re_{Lp}^{1-n}$ $Re_{Lp} = \dot{m}(1-x)D_{hp}/\mu_L$ Constants A and n are chosen to provide least-squares curve fits to the measured single-phase heat transfer data for each test surface	Mandrusiak and Carey [2] Methanol, butanol, water, R113	Vertical offset strip-fin geometry (Table 1), Turbulent annular flow, $1 \leqslant 1/X_{tt} \leqslant 60$, $1.8 \leqslant Pr_L \leqslant 8.6$
Mandrusiak and Carey [2]	$F = Pr_L^{0.296}\left[1 + \frac{3.53}{X_{tt}^{1/2}} + \frac{1.05}{X_{tt}^2}\right]^{1/2}$	Robertson [12], Nitrogen Robertson and Lovegrove [13], R11	Vertical offset strip-fin geometry (Table 1), Turbulent annular flow $0.4 \leqslant 1/X_{tt} \leqslant 20$, $Pr_L = 2$ (Table 1) $0.4 \leqslant 1/X_{tt} \leqslant 20$, $Pr_L = 2.25$ (Table 1)
Troniewski and Witczak [41]	$F = 2.62(1/X_{tt})^{0.66}(D/D_h)^{1.03}K^{0.06}$ $\alpha_L = 0.023(\lambda_L/D_h)\,Pr_L^{0.33}\,Re_L^{0.8}$ $1/X_{tt} = (\mu_V/\mu_L)^{0.1}(\rho_L/\rho_V)^{0.5}(x/(1-x))^{0.9}$ $D/D_h = H^{-0.5}(H + 1/H + 2)^{0.5}$ $K = 1$ for vertical ducts $K = H$ for horizontal ducts (H = ratio of sides in rectangular duct)	Troniewski and Witczak [41], Water	Rectangular channel (Table 2), Turbulent annular flow, $Pr_L = 1.7$
Kenning and Cooper [42]	$F = 1 + 1.8X_{tt}^{-0.79}$ $\alpha_L = 0.023(\lambda_L/D)\,Pr_L^{0.4}\,Re_L^{0.8}$ $1/X_{tt} = (\mu_V/\mu_L)^{0.1}(\rho_L/\rho_V)^{0.5}(x/(1-x))^{0.9}$	Data presented by Chen [65] but coming from other sources, water, methanol, cyclohexane, pentane, heptane, benzene	Circular tube, Turbulent annular flow

Table 4 (*Continued*)

Kenning and Cooper [42]	In the turbulent annular flow regime, $F = 1 + 1.8X_{\text{tt}}^{-0.87}$ $\alpha_L = 0.023(\lambda_L/D)\,Pr_L^{0.4}\,Re_L^{0.8}$ $1/X_{\text{tt}} = (\mu_V/\mu_L)^{0.1}(\rho_L/\rho_V)^{0.5}(x/(1-x))^{0.9}$ In the plug/churn flow regime, $F = 1 + 1.8X_{\text{tt}}^{-0.87}\,j_V^{*-0.5}$	Kenning and Cooper [42], Water	Vertical circular tube (Table 2), $1.1 \leqslant Pr_L \leqslant 1.5$, Annular correlation valuable for $0.6 \leqslant 1/X_{\text{tt}} \leqslant 40$, $j_V^* > 0.4$ with the 9.6 mm tube and for $j_V^* > 1$ with the 14 mm tube Plug flow correlation valuable for $0.6 \leqslant 1/X_{\text{tt}} \leqslant 20$ and $j_V^* \leqslant 1$ with the 14.4 mm tube
Wadekar [70]	$F = 3.2Y + 1$, with $Y = [x/(1-x)]^{3/4}\rho_{\text{red}}^{-3/8}M^{1/8}$ Valuable for $0.7 \leqslant Y \leqslant 15$	Robertson and Wadekar [34], Cyclohexane	Vertical perforated-fin geometry (Table 1), $\dot{m} = 290\ \text{kg}\cdot\text{m}^{-2}.\text{s}^{-1}$, 10.7 mm diameter vertical tube, $\dot{m} = 145, 290\ \text{kg}\cdot\text{m}^{-2}.\text{s}^{-1}$, $p = 0.15$ MPa 9 mm diameter horizontal tube, $p = 0.475$ MPa 9.6 and 14.4 mm diameter vertical tubes (Table 2) Turbulent annular flow, $1.1 \leqslant Pr_L \leqslant 8$
		Robertson and Wadekar [91], Ethanol	
		Ross et al. [92], R152 a and R13b1	
		Kenning and Cooper [42], Water	
Wattelet et al. [11]	$F = 3.37(1/X_{\text{tt}})^{0.686}$ $1/X_{\text{tt}} = (\mu_V/\mu_L)^{0.1}(\rho_L/\rho_V)^{0.5}(x/(1-x))^{0.9}$	Wattelet et al. [11], R 134a and R12	Horizontal circular tube (Table 2), Turbulent annular flow, $2 \leqslant 1/X_{\text{tt}} \leqslant 13$, $3 \leqslant Pr_L \leqslant 4$

ble 2) found that simple nucleate boiling correlations predicted relatively well their heat transfer coefficients results in single narrow tubes, in the confined bubbles flow region (see Section 6.2). Some of the most widely used nucleate boiling correlations valuable for large geometries and extensible to smaller geometries in some cases are those by Cooper [68,88,89] and Gorenflo [87]. They have been reported in Table 5. Cooper [88] used some 6000 pool boiling data points from published sources, relating to over 100 experiments. Cooper [68] used five sources for up or down flow of water in tubes, for which he identified the nucleate part. He concluded that the correlation in pool boiling can be used to give the trend of the heat transfer coefficient in nucleate flow boiling. The Gorenflo [87] procedure allows to calculate the pool boiling heat transfer coefficient. For a given fluid, it uses a base pool boiling heat transfer coefficient $\alpha_{\text{nb},0}$ at normalised conditions of $p_{\text{red}} = 0.1$, $R_a = 1$ μm, $\dot{q}_0 = 20000\ \text{W}\cdot\text{m}^{-2}$, determined by predictive methods or from data. Nevertheless, Kew and Cornwell [58] also underlined that pool boiling correlations often have no geometric components although the influence of surface angle and tube diameter for example have shown to be important. Indeed, as detailed in Section 6.1, nucleate boiling is enhanced in small channels at low wall superheats above that predicted by a pool boiling correlation. Consequently, different authors deduced that there was a need of a new correlation that accounts for the enhancement in small channels. Such correlations were proposed by Ishibashi and Nishikawa [45] (Table 3) and Tran et al. [7] (Table 2) and have been reported in Table 5. Ishibashi and Nishikawa [45] correlated all their experimental data obtained for the coalesced bubble region in various annuli, for the experimental conditions given in Table 3, using dimensionless characteristic numbers. Their correlation gives a heat transfer coefficient proportional to $\dot{q}^{2/3}s^{-2/3}$. Tran et al. [7] developed a new correlation for heat transfer in nucleate flow boiling in small circular and non circular channels. For this, they used as a data base the tests carried out by Wambsganss et al. [24], Tran et al. [6, 25] with R113 and R12 and new tests with R 134a, over a range of pressures ($0.045 \leqslant p_{\text{red}} \leqslant 0.20$) (Table 2), in circular, rectangular and square channels, by taking only the tests with $\Delta T_{\text{sat}} > 2.75$ K. Tran's correlation introduces a confinement number to account for the heat transfer enhancement in small channels due to the confinement effect. This correlation also includes surface tension, an important fluid property in small-channel flow boiling.

7.3. Correlations accounting for both heat transfer mechanisms, convective and nucleate boiling

As it has been underlined in Section 4, to evaluate the heat transfer coefficient accounting for both heat transfer mechanisms, the asymptotic model defined by Eq. (4) with $m \to \infty$, i.e., $\alpha = \max(\alpha_{\text{cv}}, \alpha_{\text{nb}})$, is the most adapted to flow boiling in small channels. In this model, the nucleate and

Table 5
Literature nucleate boiling correlations

Authors of correlations	Literature correlations
Cooper [68,88,89]	Eq. (10) with $C = 55M^{-0.5}p_{\text{red}}^{0.12}(-\log_{10} p_{\text{red}})^{-0.55}$, $n = 0.67$
Gorenflo [87]	Eq. (10) with $C = \frac{\alpha_{\text{nb},0}}{(\dot{q}_0)^{0.9-0.3p_{\text{red}}^{0.3}}}\left[1.2p_{\text{red}}^{0.27} + p_{\text{red}}\left(2.5 + \frac{1}{1-p_{\text{red}}}\right)\right]$, $n = 0.9 - 0.3p_{\text{red}}^{0.3}$
Ishibashi and Nishikawa [45]	In the coalesced bubble region, $Nu = 200\,Fo^{-2/3}\,Pr_L^{-2/3}(\rho_L/\rho_V)^{-1/2}$ where $Nu = \alpha s/\lambda_L$, $Fo = a_{\text{L}}/(Ns^2)$, $N = 1.365 \times 10^{-9}\dot{q}s^{-3/2}\,Pr_L^{1.627}(\rho_L/\rho_V)^{1.085}$, thus α proportional to $\dot{q}^{2/3}s^{-2/3}$. In the isolated bubble region, α proportional to $\dot{q}^{2/3}s^{-0.13}$
Tran et al. [7]	Eq. (10) with $C = 770\frac{\lambda_L}{D_h}\left(\frac{D_h}{L_v\mu_L}Co\right)^{0.62}\left(\frac{\rho_V}{\rho_L}\right)^{0.297}$, $n = 0.62$

Table 6
Literature correlations accounting for both heat transfer mechanisms, convective and nucleate boiling

Authors of correlations	Literature correlations	Data sources, Fluids	Geometries, test conditions
Liu and Winterton [90]	Vertical or horizontal flow (for $Fr > 0.05$): $\alpha = [(S\alpha_{\text{nb}})^m + \alpha_{\text{cv}}^m]^{1/m}$ $m = 2$ $\alpha_{\text{nb}} = 55M^{-0.5}p_{\text{red}}^{0.12}(-\log_{10} p_{\text{red}})^{-0.55}\dot{q}^{2/3}$ $S = [1 + 0.055E^{0.1}Re_{TL}^{0.16}]^{-1}$ $\alpha_{\text{cv}} = E\alpha_{TL}$ $E = [1 + x\,Pr_L(\rho_L/\rho_V - 1)]^{0.35}$ $\alpha_{TL} = 0.023(\lambda_L/D_h)\,Pr_L^{0.4}\,Re_{TL}^{0.8}$ In annuli, the heated equivalent diameter is used instead of D_h Horizontal flow and $Fr < 0.05$: $S\alpha_{\text{nb}}$ and α_{cv} should be multiplied by $\sqrt{Fr}$ and $Fr^{(0.1-2Fr)}$, respectively	Data presented by Gungor and Winterton [81] collected from 30 different literature sources involving nine different fluids	Tube or annulus, $2.95 \leqslant D_h \leqslant 32$ (mm), Turbulent liquid flow, $12.4 \leqslant \dot{m} \leqslant 8179.3$ kg·m^{-2}·s^{-1}, $348.9 \leqslant \dot{q} \leqslant 2.62 \times 10^6$ W·m^{-2}, $569 \leqslant Re_{TL} \leqslant 8.75 \times 10^5$, $0.83 \leqslant Pr_L \leqslant 9.1$
Wattelet et al. [14]	$\alpha = [\alpha_{\text{nb}}^m + \alpha_{\text{cv}}^m]^{1/m}$ $m = 2.5$ $\alpha_{\text{nb}} = 55M^{-0.5}p_{\text{red}}^{0.12}(-\log_{10} p_{\text{red}})^{-0.55}\dot{q}^{2/3}$ $\alpha_{\text{cv}} = F\alpha_L R$ $F = 1 + 1.925X_{\text{tt}}^{-0.83}$ $\alpha_L = 0.023(\lambda_L/D_h)\,Pr_L^{0.4}\,Re_L^{0.8}$ $R = 1.32\,Fr^{0.2}$ if $Fr < 0.25$ $R = 1$ if $Fr > 0.25$ $X_{\text{tt}} = (\mu_L/\mu_V)^{0.1}(\rho_V/\rho_L)^{0.5}((1-x)/x)^{0.9}$	Wattelet et al. [14], R12 and R134a	Horizontal circular tube (Table 2), Turbulent annular flow, $3 \leqslant Pr_L \leqslant 4$

convective boiling components can be evaluated by either of the correlations proposed in the two previous sections.

Besides, two recently obtained correlations using an asymptotic form with $1 < m < 3$ have been reported in Table 6. Liu and Winterton [90] successfully developed a flow boiling correlation for vertical and horizontal flow in tubes and annuli. The data used in developing their correlation are the same as those described in Gungor and Winterton [81]. They were collected from 30 different literature sources involving nine different fluids. The data bank contains 4202 data points for saturated boiling. Liu and Winterton [90] showed that the F factor should have a Prandtl number, vapour quality and ρ_L/ρ_V dependence. The Dittus–Boelter correlation was selected to evaluate α_L. The Cooper [88,89] correlation was selected for the nucleate boiling term. If the tube is horizontal and the Froude number less than 0.05, the authors included Froude number correction factors in their correlation. Compared with the saturated boiling data used in developing the equations, the new correlation is more reliable than any of the other correlations tested [63,65,80,81].

Using their experimental data on boiling heat transfer coefficient in an horizontal circular tube (Table 2), Wattelet et al. [14] modified an empirical correlation developed for annular flow data using an asymptotic form to account for the decrease in heat transfer due to wavy-stratified flow pattern in horizontal flow for low mass fluxes (see Section 5.5). The Cooper [88,89] correlation was selected for the nucleate boiling term, while for the convective boiling term, a modified form of the convective term in the Chen [65] correlation was selected. The Dittus–Boelter correlation was selected to evaluate α_L. For low mass fluxes, a Froude number correction was added to the convective boiling term to account for the decrease in available convective heat transfer area and a loss of turbulence. This correction offsets the overestimation of the single-phase liquid heat transfer coefficient through use of the Dittus–Boelter correlation for tests with Reynolds

numbers below 10 000. This correlation predicted both the annular and wavy-stratified flow data well.

8. Conclusions

Thanks to their numerous advantages (small size, low weight, low cost), compact evaporators are attractive for use in the transportation (vehicular, aircraft, airspace) industry. Even if their use has become extensive in that industry, there is always a lack of an established design methodology and accompanying data bases. At present, design advancement is made on the basis of experience and experimentation on prototype units. The process industries are also interested in use of compact heat exchangers for phase-change heat transfer applications. However, design correlations and industrial standards are lacking and are impeding their application and use.

The reviewed experimental studies, whose channel geometry/size, test conditions and fluids have been reported in Tables 1, 2 and 3 allowed to obtain information on boiling characteristics for a very large range of parameters. In parallel, as the interpretation of heat transfer mechanisms requires a knowledge of the prevailing flow regimes, the flow pattern configurations susceptible to be observed successively during flow boiling in small vertical heated channels with increasing vapour quality have been described. In addition to the usual parameters having an effect on the observed flow pattern (mass flux, heat flux, fin geometry, orientation, pressure), it has been shown that the passage dimensions have a strong effect. Especially, for test conditions corresponding to nucleate boiling dominance, whereas isolated bubbles are observed in large channels, a confined bubbles or slug flow regime is more usually observed in small channels. The typical trends of heat transfer coefficient against mass flux, vapour quality and heat flux deduced from the literature results are quite different in the two regions of boiling, nucleate and convective boiling regions. The analysis of the heat transfer mechanisms in small passages also showed that the transition between the two boiling regions was rather abrupt. Thus it is easy to distinguish between the two dominant mechanisms of boiling and determine for which range of parameters each heat transfer mechanism is predominant. Moreover, to correlate the heat transfer coefficient, the asymptotic model where the heat transfer coefficient is equal to the larger one of the convective or nucleate boiling component is the mostly adapted. The characteristics of convective and nucleate boiling in small channels, with associated flow patterns to each boiling region, have been developed separately. In particular, in the convective boiling region, the associated flow pattern is either the intermittent flow including the slug and churn flows at low mass fluxes and low vapour qualities and the non-intermittent flow including the annular flow at higher mass fluxes or vapour qualities. In this region, the parameters with the stronger influence on heat transfer and flow pattern are mass flux, vapour quality and fin geometry. Especially the use of small scale enhanced passages, like serrated or perforated plate-fin passages can substantially enhance the heat exchanger performance. In the nucleate boiling region, the associated flow pattern is either the isolated bubbles flow or the confined bubbles flow and the parameters with the stronger influence on heat transfer and flow pattern are channel dimensions and heat flux. The decrease in channel dimensions can considerably enhance the heat-exchanger performance as long as the heat flux is lower than the critical heat flux. For large channels, many literature correlations (either correlations for one of the mechanisms, nucleate or convective boiling or correlations containing two terms, one for nucleation and one for convection) are available to predict the heat transfer coefficient. At the opposite, in compact heat exchangers, validated correlations are lacking and are complicated by the strong dependence on channel size for some flow regimes. Some interesting correlations valuable for channels of small dimensions, in the nucleate boiling or convective boiling region have been reported. The reported nucleate boiling correlations express the heat transfer coefficient as a function of heat flux, fluid properties, fluid pressure and channel dimensions. Convective boiling correlations express the heat transfer coefficient as a function of fluid properties, mass flux, vapour quality and channel geometry/dimensions.

Thus, the present work has provided valuable insights and understandings of the heat transfer mechanisms and channel geometry/ size effects, among other things. Nevertheless, systematic studies are still required to generate a sufficient technology base for the development of design correlations and standards.

References

[1] V.P. Carey, G.D. Mandrusiak, Annular film-flow boiling of liquids in a partially heated vertical channel with offset strip fins, Internat. J. Heat Mass Transfer 29 (6) (1986) 927–939.
[2] G.D. Mandrusiak, V.P. Carey, Convective boiling in vertical channels with different offset strip fin geometries, ASME J. Heat Transfer 111 (1989) 156–165.
[3] K. Cornwell, P.A. Kew, Boiling in small parallel channels, in: Proc. of the Internat. Conf. on Energy Efficiency in Process Technology, Elsevier Applied Science, Athens, Greece, 1992, pp. 624–638.
[4] V.V. Wadekar, Flow boiling of heptane in a plate-fin heat exchanger passage, Compact Heat Exchangers for Power and Process Industries, HTD, Proc. of the ASME Heat Transfer Division 201 (1992) 1–6.
[5] V.P. Carey, Two-phase flow in small-scale ribbed and finned passages for compact evaporators and condensers, Nuclear Engrg. Design 141 (1993) 249–268.
[6] T.N. Tran, M.W. Wambsganss, D.M. France, J.A. Jendrzejczyk, Boiling heat transfer in a small, horizontal, rectangular channel, Heat Transfer, Atlanta, AIChE Sympos. Ser. 89 (295) (1993) 253–261.
[7] T.N. Tran, M.W. Wambsganss, M.C. Chyu, D.M. France, A correlation for nucleate flow boiling in small channels, in: Proc. of the International Conference on Compact Heat Exchangers for the Process Industries, Snowbird, Utah, 1997, pp. 353–363.
[8] R. Mertz, A. Wein, M. Groll, Experimental investigation of flow boiling heat transfer in narrow channels, in: G.P. Celata, P. Di Marco, A. Mariani (Eds.), 2nd European Thermal Sciences and 14th UIT National Heat Transfer Conference, Edizioni ETS, 1996, pp. 219–226.

[9] P.A. Kew, K. Cornwell, Correlations for the prediction of boiling heat transfer in small-diameter channels, Appl. Thermal Engrg. 17 (8–10) (1997) 705–715.
[10] H. Oh, M. Katsuta, K. Shibata, Heat transfer characteristics of R134a in a capillary tube heat exchanger, in: Proc. of 11th International Heat Transfer Conference, Vol. 6, 1998, pp. 131–136.
[11] J. Wattelet, J.M. Saiz Jabardo, J.C. Chato, J.S. Panek, A.L. Souza, Experimental evaluation of convective boiling of refrigerants HFC134a and CFC12, Two-Phase Flow and Heat Transfer, Proc. of the ASME Heat Transfer Division 197 (1992) 121–127.
[12] J.M. Robertson, Boiling heat transfer with liquid nitrogen in brazed-aluminium plate-fin heat exchangers, National Heat Transfer Conference, San Diego, AIChE Sympos. Ser. 189 (75) (1979) 151–164.
[13] J.M. Robertson, P.C. Lovegrove, Boiling heat transfer with Freon 11 in brazed aluminium plate-fin heat exchangers, ASME J. Heat Transfer 105 (1983) 605–610.
[14] J.P. Wattelet, J.C. Chato, A.L. Souza, B.R. Christoffersen, Evaporative characteristics of R12, R134a, and a mixture at low mass fluxes, ASHRAE Trans. Sympos. 100 (1994) 603–615.
[15] W.J. Yang, N.L. Zhang, Micro and nano-scale heat transfer phenomena research trends, in: Transport Phenomena Science and Technology, Higher Education Press, Beijing, 1992, pp. 1–15.
[16] C. Xia, Z. Guo, W. Hu, Mechanism of boiling heat transfer in narrow channels, Two-Phase Flow and Heat Transfer, Proc. of the ASME Heat Transfer Division 197 (1992) 111–119.
[17] X.F. Peng, B.X. Wang, Forced convection and flow boiling heat transfer for liquid flowing through microchannels, Internat. J. Heat Mass Transfer 36 (1993) 3421–3427.
[18] X.F. Peng, B.X. Wang, G.P. Peterson, H.B. Ma, Experimental investigation of heat transfer in flat plates with rectangular microchannels, Internat. J. Heat Mass Transfer 38 (1) (1995) 127–137.
[19] T. Wilmarth, M. Ishii, Two-phase flow regimes in narrow rectangular vertical and horizontal channels, Internat. J. Heat Mass Transfer 37 (12) (1994) 1749–1758.
[20] K. Moriyama, A. Inoue, H. Ohira, The thermohydraulic characteristics of two-phase flow in extremely narrow channels (The frictional pressure drop and heat transfer of boiling two-phase flow, Analytical Model), Heat Transfer—Japan. Res. 21 (8) (1992) 823–856.
[21] R.K. Shah, Classification of heat exchangers, in: S. Kakac, A.E. Bergles, F. Mayinger (Eds.), Heat Exchangers: Thermal-Hydraulic Fundamentals and Design, 1986, pp. 9–46.
[22] S. Lin, P.A. Kew, K. Cornwell, Two-phase flow regimes and heat transfer in small tubes and channels, in: Proc. of 11th International Heat Transfer Conference, Vol. 2, Kyongju, Korea, 1998, pp. 45–50.
[23] V.V. Wadekar, Vertical slug flow heat transfer with nucleate boiling, ASME HTD 159 (1991) 157–161.
[24] M.W. Wambsganss, D.M. France, J.A. Jendrzejczyk, T.N. Tran, Boiling heat transfer in a small-diameter tube, ASME J. Heat Transfer 115 (1993) 963–972.
[25] T.N. Tran, M.W. Wambsganss, D.M. France, Small circular and rectangular channel boiling with two refrigerants, Internat. J. Multiphase Flow 22 (3) (1996) 485–498.
[26] H. Panitsidis, R.D. Gresham, J.W. Westwater, Boiling of liquids in a compact plate-fin heat exchanger, Internat. J. Heat Mass Transfer 18 (1975) 37–42.
[27] V.B. Galezha, I.P. Usyukin, K.D. Kan, Boiling heat transfer with freons in finned-plate heat exchangers, Heat Transfer Soviet Res. 8 (3) (1976) 103–110.
[28] D. Yung, J.J. Lorenz, C. Panchal, Convective vaporization and condensation in serrated-fin channels, Heat Transfer in OTEC systems, Proc. of the ASME Heat Transfer Division 12 (1980) 29–37.
[29] C.C. Chen, J.W. Westwater, Application of the local assumption for the design of compact heat exchangers for boiling heat transfer, ASME J. Heat Transfer 106 (1984) 204–209.
[30] C.B. Panchal, Heat transfer with phase change in plate-fin heat-exchangers, AIChE Sympos. Series 80 (236) (1984) 90–97.
[31] J.M. Robertson, The boiling characteristics of perforated plate-fin channels with liquid nitrogen in upflow, Heat Exchangers for Two-Phase Applications, Proc. of the ASME Heat Transfer Division 10 (1983) 35–40.
[32] J.M. Robertson, R.H. Clarke, The general prediction of convective boiling coefficients in plate-fin heat exchanger passages, Heat Transfer, Denver, AIChE Sympos. Ser. 81 (245) (1985) 129–134.
[33] J.M. Robertson, P.C. Lovegrove, Boiling heat transfer with Freon 11 in brazed aluminium plate-fin heat exchangers, in: ASME/AIChe National Heat Transfer Conf. 80-HT-58, Orlando, 1980, pp. 1–8.
[34] J.M. Robertson, V.V. Wadekar, Boiling characteristics of cyclohexane in vertical upflow in perforated plate-fin passages, 25th National Heat Transfer Conference, Houston, AIChE Sympos. Ser. 84 (263) (1988) 120–125.
[35] G.D. Mandrusiak, V.P. Carey, X. Xu, An experimental study of convective boiling in a partially heated horizontal channel with offset strip fins, ASME J. Heat Transfer 110 (1988) 229–236.
[36] S. Koyama, J. Ohara, K. Kuwahara, K. Masaki, Falling film evaporation of pure refrigerant HCFC123 in a vertical rectangular channel with serrated fins, HTD, Proc. of the ASME Heat Transfer Division 361 (1) (1998) 339–346.
[37] A. Feldman, De l'ébullition en convection forcée dans des canaux d'échangeurs à plaques et ailettes, Ph.D. Thesis, Université Henri Poincaré, Nancy I, 1996.
[38] A. Feldman, C. Marvillet, M. Lebouché, Nucleate and convective boiling in plate fin heat exchangers, Internat. J. Heat Mass Transfer 43 (2000) 3433–3442.
[39] B. Watel, B. Thonon, Flow boiling in plate fin heat exchanger, in: 3rd European Thermal-Sciences Conference, Heidelberg, 2000, pp. 1171–1176.
[40] G.M. Lazarek, S.H. Black, Evaporative heat transfer, pressure drop and critical heat flux in a small vertical tube with R113, Internat. J. Heat Mass Transfer 25 (7) (1982) 945–960.
[41] L. Troniewski, S. Witczak, Heat transfer boiling flow through rectangular ducts, in: T.N. Vezirolu (Ed.), Particular Phenomena and Multiphase Transport, Hemisphere Publishing, New York, 1988, pp. 89–97.
[42] D.B.R. Kenning, M.G. Cooper, Saturated flow boiling of water in vertical tubes, Internat. J. Heat Mass Transfer 32 (3) (1989) 445–458.
[43] J.Y. Shin, M.S. Kim, S.T. Ro, Experimental study on forced convective boiling heat transfer of pure refrigerants mixtures in a horizontal tube, Internat. J. Refrig. 20 (4) (1997) 267–275.
[44] M. Kureta, T. Kobayashi, K. Mishima, H. Nishihara, Pressure drop and heat transfer for flow boiling of water in small-diameter tubes, JSME Internat. J. Ser. B Fluids Thermal Engrg. 41 (4) (1998) 871–879.
[45] E. Ishibashi, K. Nishikawa, Saturated boiling heat transfer in narrow spaces, Internat. J. Heat Mass Transfer 12 (1969) 863–894.
[46] M.K. Jensen, P.E. Cooper, A.E. Bergles, Boiling Heat Transfer and dryout in restricted annular geometries, Nuclear, Solar and Process Heat Transfer, St. Louis, AIChE Sympos. Series 73 (164) (1976) 205–214.
[47] S. Aoki, A. Inoue, M. Aritomi, Y. Sakamoto, Experimental study on the boiling phenomena within a narrow gap, Internat. J. Heat Mass Transfer 25 (7) (1982) 985–990.
[48] Y. Fujita, H. Ohta, S. Uchida, K. Nishikawa, Nucleate boiling heat transfer and critical heat flux in narrow space between rectangular surfaces, Internat. J. Heat Mass Transfer 31 (2) (1988) 229–239.
[49] R. Mertz, M. Groll, C. Marvillet, J.E. Hesselgreaves, Enhanced static evaporation heat transfer surfaces for compact two-phase heat exchangers, Heat Recovery Systems CHP 14 (5) (1994) 493–506.
[50] M. Aritomi, T. Miyata, M. Horiguchi, A. Sudi, Thermo-hydraulics of boiling two-phase flow in high conversion light water reactors (Thermo-hydraulics at low velocities), Internat. J. Multiphase Flow 19 (1) (1993) 51–63.
[51] G.D. Mandrusiak, V.P. Carey, Pressure drop characteristics of two-phase flow in a vertical channel with offset strip fins, Experimental Thermal Fluid Sci. 1 (1988) 41–50.

[52] C.A. Damianides, J.W. Westwater, Two-phase flow patterns in a compact heat exchanger and in small tubes, in: Proc 2nd UK Nat. Conf. On Heat Transfer 2, Glasgow, Scotland, 1988, pp. 1257–1268.
[53] M.W. Wambsganss, J.A. Jendrzejczyk, D.M. France, T.N. Tran, Two-phase flow patterns and transitions in a small horizontal, rectangular channel, Internat. J. Multiphase Flow 17 (3) (1991) 327–342.
[54] M.W. Wambsganss, J.A. Jendrzejczyk, D.M. France, Two-phase flow and pressure drop in flow passages of compact heat exchangers, in: Society of Automotive Engineers International Congress and Exposition, Detroit, 1992, pp. 1–19.
[55] K. Mishima, T. Hibiki, H. Nishihara, Some characteristics of gas–liquid flow in narrow rectangular ducts, Internat. J. Multiphase Flow 19 (1) (1993) 115–124.
[56] K. Mishima, T. Hibiki, Some characteristics of air–water two-phase flow in small diameter vertical tubes, Internat. J. Multiphase Flow 22 (4) (1996) 703–712.
[57] J. Xu, Experimental study on gas–liquid two-phase flow regimes in rectangular channels with mini gaps, Internat. J. Heat and Fluid Flow 20 (1999) 422–428.
[58] P.A. Kew, K. Cornwell, Confined bubble flow and boiling in narrow spaces, in: Proc. of 10th International Heat Transfer Conference, Vol. 7, Brighton, UK, 1994, pp. 473–478.
[59] K. Nishikawa, Y. Fujita, Nucleate boiling heat transfer and its augmentation, Adv. Heat Transfer 20 (1990) 1–82.
[60] M. Monde, Measurement of liquid film thickness during passage of bubbles in a vertical rectangular channel, ASME J. Heat Transfer 112 (1990) 255–257.
[61] S.G. Bankoff, T.E. Rehm, Convective boiling in narrow concentric annuli, J. Engrg. Gas Turbines Power 112 (1990) 607–613.
[62] M.M. Shah, A new correlation for heat transfer during boiling flow through pipes, ASHRAE Trans. 82 (2) (1976) 66–86.
[63] M.M. Shah, Chart correlation for saturated boiling heat transfer equations and further study, ASHRAE Trans. 88 (1) (1982) 185–196.
[64] S.G. Kandlikar, A general correlation for saturated two-phase flow boiling heat transfer inside horizontal and vertical tubes, ASME J. Heat Transfer 112 (1990) 219–228.
[65] J.C. Chen, Correlation for boiling heat transfer to saturated fluids in convective flow, I&EC Process Design and Development 5 (3) (1966).
[66] D. Steiner, J. Taborek, Flow boiling heat transfer in vertical tubes correlated by an asymptotic model, Heat Transfer Engrg. 13 (2) (1992) 43–69.
[67] R.L. Webb, N.S. Gupte, A critical review of correlations for convective vaporization in tubes and tube banks, Heat Transfer Engrg. 13 (3) (1992) 58–81.
[68] M.G. Cooper, Flow boiling—The 'apparently nucleate' regime, Internat. J. Heat Mass Transfer 32 (3) (1989) 459–464.
[69] V.V. Wadekar, D.B.R. Kenning, Flow boiling heat transfer in vertical slug and churn region, in: Proc. of 9th international Heat Transfer Conference, Vol. 3, 1990, pp. 449–454.
[70] V.V. Wadekar, Flow boiling—A simple correlation for convective heat transfer component, in: Proc. of 9th International Heat Transfer Conference, Vol. 2, Jerusalem, 1990, pp. 87–91.
[71] V.V. Wadekar, K. Tuzla, J.C. Chen, Heat transfer to air–water two-phase flow in slug/churn region, National Heat Transfer Conference, Proc. of the ASME Heat Transfer Division 326 (1996) 219–225.
[72] K.W. McQuillan, P.B. Whalley, Flow patterns in vertical two-phase flow, Internat. J. Multiphase Flow 11 (1985) 161–175.
[73] V.P. Carey, Surface tension effects on convective boiling heat transfer in compact heat exchangers with offset-strip fins, ASME J. Heat Transfer 107 (1985) 970–974.
[74] R.K. Shah, A.L. London, Laminar Flow Forced Convection in Ducts, Academic Press, New York, 1978.
[75] A.R. Wieting, Empirical correlations for heat transfer and flow friction characteristics of rectangular offset-fin plate-fin heat exchangers, ASME J. Heat Transfer 97 (1975) 488–490.
[76] M. Monde, Characteristic of heat transfer enhancement due to bubbles passing through a narrow vertical channel, ASME J. Heat Transfer 110 (1988) 1016–1019.
[77] M. Monde, Y. Mitsutake, Enhancement of heat transfer due to bubbles passing through a narrow vertical rectangular channel, Internat. J. Multiphase Flow 15 (5) (1989) 803–814.
[78] A. Bar-Cohen, H. Schweitzer, Thermosyphon boiling in vertical channels, ASME J. Heat Transfer 107 (1985) 773–778.
[79] D.L. Bennett, J.C. Chen, Forced convective boiling in vertical tubes for saturated pure components and binary mixtures, AICHE J. 26 (3) (1980) 454–461.
[80] K.E. Gungor, R.H.S. Winterton, A general correlation for flow boiling in tubes and annuli, Internat. J. Heat Mass Transfer 29 (1986) 351–358.
[81] K.E. Gungor, R.H.S. Winterton, Simplified general correlation for saturated flow boiling and comparisons of correlations with data, Chem. Engrg. Res. Des. 65 (1987) 148–156.
[82] M.R. Aligoodarz, D.B.R. Kenning, Vapour bubble behaviour in a single narrow channel, Proc. 4th UK National Conf. on Heat Transfer, Manchester, UK, 1995, pp. 273–276.
[83] C.N. Ammerman, S.M. You, Enhanced convective boiling of FC-87 in small, rectangular, horizontal channels: Heat transfer coefficient and CHF, in: AIAA/ASME Joint Thermophysics and Heat Transfer Conference, Vol. 4, ASME publications-HTD, 1998, pp. 225–233.
[84] I.I. Chernobyl'skii, I.U.M. Tananaiko, Heat exchange during boiling of liquids in narrow annular tubes, Soviet Phys. Technical Phys. (1956) 1244–1249.
[85] Y. Fujita, S. Uchida, Boiling heat transfer and critical heat flux in a confined space: Effects of gap, size, inclination angle and peripheral conditions at the space edge, in: Proc. 9th International Heat Transfer Conf., Vol. 2, 1990, pp. 153–158.
[86] K. Stephan, M. Abdelsalam, Heat transfer correlations for natural convection boiling, Internat. J. Heat Mass Transfer 23 (1980) 73–87.
[87] D. Gorenflo, Behältersieden, Sec. Ha, in VDI Wärmeatlas, VDI Verlag, Düsseldorf, 1997.
[88] M.G. Cooper, Saturated nucleate pool boiling—A simple correlation, 1st UK National Conference on Heat Transfer, Leeds, UK, ICHEME Sympos. Ser. 2 (86) (1984) 785–793.
[89] M.G. Cooper, Heat flow rates in saturated nucleate pool boiling—A wide-ranging correlation using reduced properties, Adv. Heat Transfer 16 (1984) 158–239.
[90] Z. Liu, R.H.S. Winterton, A general correlation for saturated and subcooled flow boiling in tubes and annuli, based on a nucleate pool boiling equation, Internat. J. Heat Mass Transfer 34 (11) (1991) 2759–2766.
[91] J.M. Robertson, V.V. Wadekar, Vertical upflow boiling of ethanol in a 10 mm diameter tube, in: Proc. 2nd UK National Heat Transfer Conference, Vol. 1, Glasgow, 1988, pp. 66–77.
[92] H. Ross, R. Radermacher, M. di Marzo, D. Didion, Horizontal flow boiling of pure and mixed refrigerants, Internat. J. Heat Mass Transfer 30 (1987) 979–992.